Review of Literature on Heat Transfer Enhancement in Compact Heat Exchangers

K. M. Stone

ACRC TR-105 August 1996

For additional information:

Air Conditioning and Refrigeration Center
University of Illinois
Mechanical & Industrial Engineering Dept.
1206 West Green Street
Urbana, IL 61801

(217) 333-3115

Prepared as part of ACRC Project 65
Investigation of Wavy Fins for Heat Transfer
Augmentation in Refrigeration/Air Conditioning Systems
A. M. Jacobi, T. A. Newell and S. P. Vanka, Principal Investigators

The Air Conditioning and Refrigeration Center was founded in 1988 with a grant from the estate of Richard W. Kritzer, the founder of Peerless of America Inc. A State of Illinois Technology Challenge Grant helped build the laboratory facilities. The ACRC receives continuing support from the Richard W. Kritzer Endowment and the National Science Foundation. The following organizations have also become sponsors of the Center.

Amana Refrigeration, Inc.
Brazeway, Inc.
Carrier Corporation
Caterpillar, Inc.
Dayton Thermal Products
Delphi Harrison Thermal Systems
Eaton Corporation
Ford Motor Company
Frigidaire Company
General Electric Company
Lennox International, Inc.
Modine Manufacturing Co.
Peerless of America, Inc.
Redwood Microsystems, Inc.
U. S. Army CERL
U. S. Environmental Protection Agency
Whirlpool Corporation

For additional information:

Air Conditioning & Refrigeration Center
Mechanical & Industrial Engineering Dept.
University of Illinois
1206 West Green Street
Urbana IL 61801

217 333 3115

REVIEW OF LITERATURE ON HEAT TRANSFER ENHANCEMENT IN COMPACT HEAT EXCHANGERS

written by Kevin Stone
under supervision of Prof. S. Pratap Vanka

ABSTRACT

This paper features a broad discussion on the application of enhanced heat transfer surfaces to compact heat exchangers. The motivation for heat transfer enhancement is discussed, and the principles behind compact heat exchangers are summarized. Next, various methods for evaluating and comparing different types of heat transfer enhancement devices using first and/or second law analysis are presented. Finally, the following plate-fin enhancement geometries are discussed: rectangular and triangular plain fins, offset strip fins, louvered fins, and vortex generators.

MOTIVATION FOR HEAT TRANSFER ENHANCEMENT

For well over a century, efforts have been made to produce more efficient heat exchangers by employing various methods of heat transfer enhancement. The study of enhanced heat transfer has gained serious momentum during recent years, however, due to increased demands by industry for heat exchange equipment that is less expensive to build and operate than standard heat exchange devices. Savings in materials and energy use also provide strong motivation for the development of improved methods of enhancement. When designing cooling systems for automobiles and spacecraft, it is imperative that the heat exchangers are especially compact and lightweight. Also, enhancement devices are necessary for the high heat duty exchangers found in power plants (i. e. air-cooled condensers, nuclear fuel rods). These applications, as well as numerous others, have led to the development of various enhanced heat transfer surfaces.

In general, enhanced heat transfer surfaces can be used for three purposes: (1) to make heat exchangers more compact in order to reduce their overall volume, and possibly their cost, (2) to reduce the pumping power required for a given heat transfer process, or (3) to increase the overall UA value of the heat exchanger. A higher UA value can be exploited in either of two ways: (1) to obtain an increased heat exchange rate for fixed fluid inlet temperatures, or (2) to reduce the mean temperature difference for the heat exchange; this increases the thermodynamic process efficiency, which can result in a saving of operating costs.

Enhancement techniques can be separated into two categories: passive and active. Passive methods require no direct application of external power. Instead, passive techniques employ special surface geometries or fluid additives which cause heat transfer enhancement. On the other hand, active schemes such as electromagnetic fields and surface vibration do require external power for operation [1].

The majority of commercially interesting enhancement techniques are passive ones. Active techniques have attracted little commercial interest because of the costs involved, and the problems that are associated with vibration or acoustic noise [2]. This paper deals only with gas-side heat transfer enhancement using special surface geometries.

Special surface geometries provide enhancement by establishing a higher hA per unit base surface area. Clearly, there are three basic ways of accomplishing this [2]:

1. Increase the effective heat transfer surface area (A) per unit volume without appreciably changing the heat transfer coefficient (h). Plain fin surfaces enhance heat transfer in this manner.

2. Increase h without appreciably changing A. This is accomplished by using a special channel shape, such as a wavy or corrugated channel, which provides mixing due to secondary flows and boundary-layer separation within the channel. Vortex generators also increase h without a significant area increase by creating longitudinally spiraling vortices exchange fluid between the wall and core regions of the flow, resulting in increased heat transfer [3].

3. Increase both h and A. Interrupted fins (i. e. offset strip and louvered fins) act in this way. These surfaces increase the effective surface area, and enhance heat transfer through repeated growth and destruction of the boundary layers.

COMPACT HEAT EXCHANGERS

In forced-convection heat transfer between a gas and a liquid, the heat transfer coefficient of the gas may be 10 to 50 times smaller than that of the liquid. The use of specially-configured surfaces can be used to reduce the gas-side thermal resistance. For heat transfer between two gases, the difficulty in inducing the desired heat exchange is even more pronounced. In this case especially, the use of enhanced surfaces can substantially reduce heat exchanger size. This is the motivation behind the design of a category of heat exchangers with reduced size and greatly enhanced gas-side heat transfer, which are referred to as "compact".

A compact heat exchanger is generally defined as one which incorporates a heat transfer surface having a high "area density". In other words, it possesses a high ratio of heat transfer surface area to volume. This does not necessarily mean that a compact heat exchanger is of small mass or volume. Figure 1 shows a large plate-fin heat exchanger matrix with high area density. Several of these units can be incorporated into a large, complicated heat exchange unit like the one shown in Figure 2. From Figures 1 and 2, it is evident that "compact" and "small" are not equivalent. However, if compact heat exchangers did not incorporate a surface of such high area density, the resulting units would be much more bulky and massive than their compact counterparts.

Quantitatively, Shah [4] arbitrarily defines a compact heat exchange surface as one that has an area density (β) greater than 700 m^2 / m^3 (213 ft^2 / ft^3). Figure 3 shows a spectrum of surface area density for heat exchangers. The range of surface area density (and hydraulic diameter) is given for various types of heat exchange surfaces, with the dividing line for compactness clearly marked.

Compact surfaces are used to yield a specified heat exchanger performance $q/\Delta T_{mean}$, within acceptable mass and volume constraints, where

$$\frac{q}{\Delta T_{mean}} = U\beta V \qquad (1)$$

From Equation 1, it is obvious that a high β decreases volume. Furthermore, compact surfaces generally result in higher overall conductance, U. And since compact surfaces can achieve structural strength and stability with thinner sections, the reduction in heat exchanger mass is even more pronounced than the reduction in volume [4].

Various techniques can be used to make heat exchangers more compact. Figure 4 shows three general types of extended surface geometries which can be used to increase gas-side heat transfer coefficients. These include: (a) a finned-tube heat exchanger with flat fins, (b) a finned-tube heat exchanger with individually finned tubes, and (c) a plate-fin heat exchanger. This paper focuses on various types of plate-fin geometries.

A typical element of a plate-fin heat exchanger consists of a die-formed fin plate sandwiched between flat metal separator plates as shown in Figures 5 and 6. Side bars are located along the outer edges of the fin sections. Stacks of such elements are then welded or dip-brazed to form large heat exchange devices like those in Figures 1 and 2. A wide variety of plate-fin geometries have been used to obtain enhanced heat transfer, and engineers are constantly working to develop new and more effective enhanced surfaces. Six commonly used plate-fin geometries are shown in Figure 7.

Typical fin spacings are 300 to 800 fins / m. Due to their small hydraulic diameter and the low density of gases, these surfaces are usually operated in the Reynolds number range $500 < Re < 1500$ [2]. As a result, plate-fin enhancement geometries must be effective in the low Reynolds number regime. For example, surface roughness has been shown to promote heat transfer in the turbulent regime, but it does not provide appreciable enhancement in the lower Reynolds number range.

EVALUATION OF HEAT TRANSFER ENHANCEMENT

When one is looking for a special surface geometry to enhance heat transfer in an industrial heat exchange application, one has a large number of options to choose from. How can one compare the performance improvement given by various enhanced surfaces? Certainly, one can judge the relative heat transfer enhancement for selected geometries by comparing the heat transfer coefficients, or dimensionless heat transfer parameters (i. e. Nusselt number, Stanton number, etc.) yielded by each enhanced surface. But this will only give a partial indication of performance. Enhanced surfaces do provide a greater heat transfer coefficient, but they also lead to increased fluid flow friction and pressure drop. Sometimes, the benefits gained from heat transfer enhancement are not great enough to offset the increased friction losses. Clearly, then, the performance goal is to gain maximum enhancement of heat transfer with minimum penalty on pumping power. However, this balance is difficult to quantify in a manner that allows straightforward comparisons between various enhanced surface geometries.

Numerous methods have been suggested to accurately evaluate the performance improvement provided by enhancement techniques. This paper provides a broad, but by no means comprehensive, look at some of the proposed procedures for judging and comparing the effecitveness of surfaces that can provide heat transfer enhancement in compact heat exchangers.

j and f vs. Curves

The basic performance data for an enhanced surface are often shown as curves of the Colburn factor ($j = St\,Pr^{2/3}$), and the Fanning friction factor (f), plotted versus Reynolds number. Kays and London [5] present j and f vs. Re for a large number of compact surfaces, in one of the

first comprehensive collections of data on enhanced surfaces for compact heat exchangers. Among the surfaces featured are the 33 plate-fin surfaces listed in the table shown in Figure 8.

Since that time, j and f curves have become a customary tool for presenting performance data for heat transfer surface geometries. However, the curves for j and f plotted vs. Re tend to vary over a wide range, in magnitude as well as slope [6], making comparisons among different geometries difficult. This fact suggests plotting j and f as functions of a parameter other than Re.

It has long been acknowledged that the flow length between boundary layer disturbances has an effect on the performance of a heat transfer surface [5], [7]. Kays and London [5] wrote: "One of the most widely used ways of increasing conductance is to interrupt the wall surfaces so that the boundary layers can never become thick." From this principle, plotting the factors j and f versus the ratio of the flow length between major boundary layer disturbances to the equivalent diameter (l/D_{eq}) is the next logical step. Kays and London [5] presented j and f vs. l/D_{eq} plots for many of the previously-mentioned compact heat transfer surfaces. Representative j and f vs. l/D_{eq} plots provided by LaHaye, *et al.* [6] are shown in Figures 9 and 10. For the heat transfer test data in Figure 9, definite trends are visible, but there is a large scattering in the data. The tested friction factors shown in Figure 10 are even more widely scattered than the heat transfer data, and the slope exponents for f do not even exhibit a visible trend. This leads one to conclude that plotting j and f vs. l/D_{eq} does not serve as a useful criterion.

"Goodness" Factors

The failure of j and f curves to portray the relative performance of heat transfer surfaces in a satisfactory fashion has led to the development of other performance parameters. Two such parameters are the "area goodness" comparison [8] and the "volume goodness" comparison [8], [9].

Area Goodness Factor

The "area goodness" method actually makes a direct comparison between j and f values, since it consists of plotting

$$j/f \text{ vs. } Re \tag{2}$$

where the flow area goodness factor (j / f) is given by

$$\frac{j}{f} = \frac{Nu\,Pr^{-1/3}}{f\,Re} = \frac{1}{A_c^2}\left[\frac{Pr^{2/3}}{2g_c\rho}\frac{NTU\cdot W^2}{\Delta p}\right] \tag{3}$$

where: A_c = core free flow area

W = fluid mass flow rate through the duct, $\rho u_m A_c$ (lbm / hr or kg / s)

For fully developed laminar flow of a specified fluid, j / f is constant for a given surface, regardless of Reynolds number. The right-hand side of Equation 3 shows that j / f is inversely proportional to A_c^2 when the bracketed quantities are constant. Therefore, a higher j / f is considered desirable because it means that a lower flow area, and thus, a lower frontal area, is required for the heat exchanger. Because j and f are both dimensionless quantities, they are independent of the hydraulic diameter (D_h). Therefore, when the area goodness factor j / f is compared for different surfaces, it reveals the influence of the cross-sectional shape regardless of the scale of the geometry [10].

Volume Goodness Factor

A comparison of surface geometries in terms of core volume is provided by plotting

$$h_{std} \text{ vs. } E_{std} \tag{4}$$

where: h_{std} = heat transfer coefficient at a standard set of fluid properties
($W / (m^2 - K)$, $Btu / (hr - ft^2 - {}^oF)$)
E_{std} = flow-friction power per unit area for a standard set of fluid properties
(W / m^2, hp / ft^2)

h_{std} is referred to as the "volume goodness factor". Expressions for h_{std} and for E_{std} are given in Equations 5 and 6:

$$h_{std} = \frac{k}{D_h} Nu = \frac{c_p \mu}{Pr^{2/3}} \frac{1}{D_h} jRe \tag{5}$$

$$E_{std} = \frac{W \Delta p}{\rho A} = \frac{\mu^3}{2 g_c \rho^2} \frac{1}{D_h^3} f Re^3 = u^m r^h \frac{\Delta p}{L} \tag{6}$$

The dimensionless heat transfer in a heat exchanger is measured by the exchanger effectiveness (ε), which is dependent on the number of transfer units (NTU) for fixed flow rates. In a "balanced" heat exchanger, the thermal resistances of both sides of the heat exchanger are of the same order of magnitude. This means that NTU is proportional to hA (or h_{std} A) for the side of the heat exchanger that is under examination. As a result, a higher h_{std} for a given E_{std} will yield a lower heat transfer area (A) for the specified exchanger effectiveness [10]. Consequently, a high position on the h_{std} vs. E_{std} plot signifies a desirable surface geometry. And, since

$$A = \beta V = (4\sigma / D_h) V \tag{7}$$

where: σ = dimensionless ratio of free flow area to frontal flow area in a heat exchanger

a high h_{std} will yield a smaller heat exchanger volume at a given E_{std} for constant σ and D_h.

Advantages and Disadvantages of Goodness Factors

Extra difficulties do exist in using the goodness factors when comparing surface geometries. For example, the area goodness factor is a useful parameter only when comparing surfaces for a fixed fluid pressure drop. With the volume goodness criterion, it is evident for Equations 5 and 6 that h_{std} and E_{std} are strongly dependent on hydraulic diameter, unlike the area goodness factor (j / f). Thus, hydraulic diameters must be fixed in order to obtain a valid volume goodness comparison. Furthermore, a representative set of fluid properties must be selected for this method. And, Cowell [11] points out that neither goodness comparison is fully quantitative.

Even London [8] admits, "These surface goodness factors are not infallible." Nevertheless, the goodness factors can provide valuable preliminary information about the relative performance of different heat transfer surfaces. As Shah and London [10] state, "These factors are easy to understand and apply, and may serve a function of screening the selection of surfaces before other design criteria are applied."

"Performance Parameters"

In order to overcome the problems associated with j and f curves, LaHaye, *et al.* [6] developed two new dimensionless groups. These two parameters are the "heat transfer performance factor" (J) and the "pumping power factor" (F) as defined by Equations 8 and 9, respectively.

$$J = (\beta h)\frac{Pr^{2/3}}{\beta c_p}\frac{D_{eq}}{\mu} = jRe \tag{8}$$

$$F = \frac{P}{V}\frac{2g_c\rho^2}{\beta}\frac{D_{eq}^3}{\mu^3} = fRe^3 \tag{9}$$

Plotting the heat transfer performance factor vs. the pumping power factor yields a "dimensionless performance plot," like the example plot shown in Figure 11. This plot also has the Reynolds number plotted on top of the performance line. Using performance plots like the one in Figure 11 for a number of surfaces, LaHaye, *et al.* [6] then attempt to create a single "idealized" performance plot which can be used to analyze all surface geometries.

Here, they use the "flow length between major boundary disturbances" (l / D_{eq}) as the varying parameter, for reasons specified previously. Eighty-three surfaces presented by Kays and London [5] were analyzed by LaHaye, *et al.* [6] using the same type of performance plot that is shown in Figure 11. From this analysis, the J factor at $F = 10^9$ (J_{10^9}) and the slope exponent (n) for all eighty-three surfaces were plotted versus l / D_{eq}, resulting in the curves shown in Figure 12. Clear trends are evident from the curves in this figure. The scattering of the points is relatively small, as is the number of "runaway" points.

The curves for J_{10^9} and n in Figure 12 were drawn taking into account the fact that they must level out at infinitely large l / D_{eq} [6]. These two curves now allow the design of the "idealized dimensionless performance plot," shown in Figure 13. This figure is a general performance plot which can be used for practically any surface geometry in the turbulent regime.

For the same D_{eq} and β, J is proportional to the heat transfer per unit volume (β_h) and F is proportional to the pumping power per unit volume, P / V. Therefore, the idealized plot shown in Figure 13 can be used to compare the effect of l on heat transfer surface performance at the same D_{eq} and β. Also, it is possible to predict the approximate performance of untested geometries or surface modification using the idealized plot, when the appropriate l has been established [6].

The idealized performance plot provides a convenient method for comparing various heat transfer geometries for a given application using only one figure. And, although the data used here encompasses only the turbulent flow range, it is believed that a similar approach can also be used for the laminar region [6]. When using the idealized performance plot for any application, however, LaHaye, *et al.* [6] note that this method should be used only as "an approximate presentation which guides the designer in the vicinity of optimum solutions," since the effects of certain parameters (most notably fin thickness) have not been accounted for.

Method for Ranking Performance of Plate-Fin Surfaces

Soland, *et al.* [12] modified the performance evaluation method of LaHaye, *et al.* [6] in comparing the performance of all the plate-finned surfaces of Kays and London [5] listed in

Figure 8, as well as various unfinned surfaces and sand-roughened surfaces [13]. The performance of all these surfaces are compared for the following quantities being equal:

1. flow rate, ω
2. hot fluid inlet temperature, $T_{h,\,in}$
3. cold fluid inlet temperature, $T_{c,\,in}$

The j and f data provided by Kays and London [5] refer to the total heat transfer area (A_T) as a function of Re based on the minimum free flow area (A_c). The comparison method proposed by Soland, *et al.* [12] converts the j and f data to j_n and f_n, which are based on the base plate area (A_b) rather than the total transfer area (A_T). Furthermore, the new Reynolds number (Re_n) is based on the open flow area (A_F), rather than on A_c. The table in Figure 14 gives the new parameter definitions proposed by Soland, *et al.* [12] compared with those used by Kays and London [5].

After making these data conversions, Soland, *et al.* [12] then used the j_n and f_n vs. Re_n data to construct performance curves using parameters similar to those proposed by LaHaye, *et al.* [6].

As previously mentioned, NTU is proportional to ha (or h_nA in this case) for the side of the heat exchanger that is under examination, if fluid properties and flow rate are held constant. Since the relationship between heat exchanger effectiveness (ε) and NTU is always monotonically increasing as shown in Figure 15, and the heat transfer for any heat exchanger is given by:

$$q = \varepsilon(T_{h,in} - T_{c,in})\omega c_p \tag{10}$$

knowledge of either NTU or h_nA allows determination of the heat transfer rate.

Hence, the parameters $\frac{NTU}{V}$ and $\frac{h_nA}{V}$ are quantities of interest, where

$$\frac{NTU}{V} = \frac{h_nA}{V\omega c_p} = \frac{4\mu}{Pr^{2/3}}\frac{j_n Re_n}{\omega D_n^2} \alpha \frac{j_n Re_n}{D_n^2} \tag{11}$$

This proportionality holds because of the fact that c_p, μ, Pr, and ω are all constant for heat exchangers using the same fluid, flow rate, and temperature levels. Similarly,

$$\frac{h_nA}{V} = \frac{4c_p\mu}{Pr^{2/3}}\frac{j_n Re_n}{D_n^2} \alpha \frac{j_n Re_n}{D_n^2} \tag{12}$$

From the proportionalities in Equations 11 and 12, $\frac{j_n Re_n}{D_n^2}$ is chosen as a heat transfer performance parameter.

Also, the pumping power per unit volume for one side of a heat exchanger is given by:

$$\frac{P}{V} = \frac{\omega \Delta p_f}{\rho V} = \frac{2\mu^3}{g_c \rho^2}\frac{f_n Re_n^3}{D_n^4} \alpha \frac{f_n Re_n^3}{D_n^4} \tag{13}$$

since μ and ρ are constant for the same fluid properties and temperature levels. From the proportionality in Equation 13, $\frac{f_n Re_n^3}{D_n^4}$ is chosen as a pumping power performance parameter. Note that the performance parameters chosen by Soland, *et al.* [12], $\frac{j_n Re_n}{D_n^2}$ and $\frac{f_n Re_n^3}{D_n^4}$, are very similar to the performance factors j Re and f Re^3 of LaHaye, *et al.* [6]. Here, however, the assumption of equal D_{eq}'s for the surfaces being examined has been eliminated.

Once the performance parameters have been calculated, $\frac{j_n Re_n}{D_n^2}$ vs. $\frac{f_n Re_n^3}{D_n^4}$ curves such as those shown in Figure 16 can be plotted for each surface that is being evaluated. A point 0 has been selected on surface 1 in Figure 16, representing a reference heat exchanger with the following properties: P_o, NTU_o, q_o, L_o, $A_{F,o}$, and V_o, where the subscript 0 refers to surface 1. The shape of the reference exchanger is labeled 0 in Figure 17. Four different comparisons can be made using the performance parameter curves shown in Figure 16 for the two sample surfaces. These four cases are indicated by points a, b, c, and d on surface 2, and correspond to the following conditions:

Case a. Same heat exchanger shape and volume. ($L_a = L_o$, $V_a = V_o$, $A_{F,a} = A_{F,o}$)
Case b. Same heat exchanger volume and pumping power. ($V_b = V_o$, $P_b = P_o$)
Case c. Same pumping power and number of transfer units. ($P_c = P_o$, $NTU_c = NTU_o$ (or $q_c = q_o$))
Case d. Same volume and number of transfer units. ($V_d = V_o$, $NTU_d = NTU_o$ (or $q_d = q_o$))

The relative heat exchanger shapes that result for the four sample comparisons are shown in Figure 17, and graphical results for the four cases are shown in Figure 18.

Thus, it is demonstrated that one can make useful performance comparisons between two heat exchangers for four different criteria using the plot of $\frac{j_n Re_n}{D_n^2}$ vs. $\frac{f_n Re_n^3}{D_n^4}$. In general, the higher a surface's curve lies on this plot, the better the surface performance. Nevertheless, Soland, *et al.* [12] advise, "The designer may not always choose this best surface since he must consider the shape of the space envelope available, costs of surfaces, and entrance and exit losses in short path length designs." Although Soland, *et al.* focused on plate-fin surfaces, this method can be applied for any type of heat exchanger surface.

First Law "Performance Evaluation Criteria" (PEC)

Bergles, Blumenkrantz, and Taborek [14], [15], Bergles, Bunn, and Junkhan [16], and Webb [17], [2] have all used first law analysis to create "performance evaluation criteria" (PEC) which can be used to compare several augmentation techniques, based on various design constraints.

Introduction to "PEC"

Bergles, Blumenkrantz, and Taborek [14], [15] establish a systematic performance evaluation procedure for enhanced heat transfer surfaces used with single-phase fluids. A summary of the eight PEC proposed by Bergles, *et al.* [14], [15] is provided by the table in Figure

19. Note that Criteria 3, 4, and 5 are conceptually equivalent to cases b, d, and c of Soland, *et al.* [12].

For the PEC given here, two constraints out of the five shown in Figure 19 are imposed for each criterion (three for Criterion 8), and then a "performance ratio" is developed to show the enhancement provided by an augmented surface relative to an unaugmented surface for one of the following performance objectives:

1. Increased heat transfer
2. Reduced pumping power
3. Reduced heat exchanger size

These performance ratios were developed assuming constant ΔT between the hot and cold fluids, and negligible thermal resistance external to the surface under consideration ($R_{ext} = 0$).

When the performance goal is increased heat transfer (Criteria 1, 2, and 3), then the corresponding performance ratios are given by:

$$R_{1,2,3} = \frac{q_a}{q_o} = \frac{h_a}{h_o} \tag{14}$$

with the appropriate parameters held constant as designated by the specific criterion in question, and by the general assumptions stated above. For all of the performance ratios, the subscript "a" refers to the augmented surface being evaluated, and the subscript "o" refers to a plain, unaugmented reference surface.

Similarly, when the performance objective is reduced pumping power (Criterion 4), the performance ratio is given by:

$$R_4 = \left(\frac{P_a}{P_o}\right)_{R_{ext}=0,D_i,L,N,q,T_{in},\Delta T} \tag{15}$$

Finally, when the performance objective is reduced heat exchanger size (Criteria 5, 6, 7, and 8), the performance ratio is given by:

$$R_{5,6,7,8} = \frac{A_a}{A_o} = \frac{h_o}{h_a} \tag{16}$$

with the appropriate parameters held constant in each case. From the definitions of the above criteria, the performance ratios can be evaluated as follows:

I) The *higher* R_1, R_2, or R_3, the more heat duty can be transferred under the given system constraints.
ii) The *lower* R_4, the lower the pumping power needed for a particular application.
iii) The *lower* R_5, R_6, R_7, or R_8, the lower the heat transfer area required for a particular service.

Bergles, Bunn, and Junkhan [16] expand on the study of PEC conducted by Bergles, Blumenkrantz, and Taborek [14], [15] by removing the assumption of constant ΔT between the hot and cold fluids, and by including the effects of thermal resistances external to the enhanced

surfaces. This extended analysis is conducted for Criteria 1, 2, 3, and 4. These criteria are applied for three cases (a, b, and c), as shown in Figure 20. For each criterion, the three cases are as follows:

Case a) Exactly the same as the corresponding criteria presented by Bergles, Blumenkrantz, and Taborek [14], [15]. Here, ΔT between the hot and cold fluids is assumed to be constant, and R_{ext} is assumed to be 0.
Case b) The assumption of constant driving temperature difference is removed.
Case c) Same as Case b, except now R_{ext} is taken into account.

For Criteria 1, 2, or 3:

$$R_{(1,2,3)a} > R_{(1,2,3)b} > R_{(1,2,3)c} \qquad (17)$$

For Criteria 4:

$$R_{4a} < R_{4b} < R_{4c} \qquad (18)$$

Equations 17 and 18 show the results of removing assumptions that can lead to overestimation of the level of enhancement provided by augmented surfaces.

In general, the PEC discussed here can be used for preliminary guidance in selecting enhanced surfaces for single-phase flow. Bergles, Bunn, and Junkhan [16] conclude,

> The presentation of heat exchanger data in terms of performance ratios permits a rapid assessment of superior heat transfer performance. Once such plots are prepared for candidate turbulence promotors *[sic]* or heat exchanger cores, the final choice can be based on other factors such as cost, susceptibility to fouling, durability, etc.

Performance Evaluation Criteria based on various geometry constraints

Webb [17] presents "a comprehensive treatise on Performance Evaluation Criteria (PEC) to assess the performance advantages offered by enhanced heat transfer surfaces." Although the PEC presented in this work are specifically applicable to single-phase flow in tubes, these PEC can also be interpreted for plate-fin heat exchangers , using Table 1 as a guideline. However, I will present the PEC as defined by Webb [17], [2] for single-phase internal tubular flow.

Webb [17] developed detailed equations for quantifying performance benefits, and gives step-by-step procedures for solution of the equations. Modified equations for internally-finned tubes are included, as well. Also, the procedure for using PEC to select "optimum" dimensions for enhanced surfaces is outlined.

Table 1 Interpretation of PEC for plate-fin geometries

Variable	Flow in Tubes	Plate-fin Geometries
Flow area	SN	S_f
Mass flow rate (W)	SNG	$SG = S_f G_f$
Surface Area	πdNL	βV
W / W_p	$\frac{N}{N_p}\frac{G}{G_p}$	$\frac{\sigma}{\sigma_p}\frac{S_f}{S_f p}\frac{G}{G_p}$

Section 17.2 of Webb [2] serves as a useful (and slightly updated) summary of the material presented in the aforementioned paper [17], but without the same detailed development and presentation of equations. The rest of the current section is dedicated to presenting material on PEC covered by Webb in Reference [2].

The premise behind this evaluation procedure is similar to that of Bergles, Blumenkrantz, and Taborek [14], [15], and Bergles, Bunn, and Junkhan [16]. This method sets a performance objective and calculates performance improvement relative to a reference design for a given set of operating conditions and design constraints, thereby defining the improvement of the objective function relative to an unenhanced heat exchanger.

The performance objectives addressed by Webb are as follows:

1. Reduced heat transfer surface material for fixed heat duty and pressure drop
2. Increased UA, which may be exploited in two ways:
   a. To obtain increased heat duty
   b. To reduce LMTD for fixed heat duty
3. Reduced pumping power for fixed heat duty

Objectives 1 and 2a are aimed at reducing heat exchanger size and capital costs, whereas Objectives 2b and 3 focus on reducing the operating costs of the heat exchanger. The major operational variables that affect the accomplishment of these goals include: heat transfer rate, pumping power (or pressure drop), heat exchanger flow rate, and fluid velocity. A PEC is established by selecting one of the operational variables as the performance objective, subject to design constraints on the remaining variables.

The four performance objectives above (1, 2a, 2b, and 3) are applied to twelve cases of interest, as shown in Figure 21. These cases pertain to flow inside enhanced and smooth tubes for equal envelope diameter. "N" refers to the number of tubes in each heat exchange pass, and the subscript "p" refers to a smooth unenhanced reference tube.

The twelve cases include three different types of constraints on the geometry of the heat exchanger:

Fixed Geometry Criteria (FG) The cross-sectional envelope area and tube length are held constant. The FG criteria usually implies a retrofit application, where there is a one-for-one replacement of plain surfaces with enhanced surfaces of the same basic geometry.

Fixed Flow Area Criteria (FN) Flow frontal area is fixed, leaving the length of the heat exchanger as a variable.

Variable Geometry Criteria (VG) This corresponds to cases where a heat exchanger is "sized" for a required thermal duty with a specified flow rate. Maintenance of a constant flow rate avoids the penalty of operating at higher thermal effectiveness encountered in the FG and FN cases.

Employment of the twelve PEC cases developed by Webb "provides a method of screening the various enhancement techniques to identify those offering greatest potential." [17]

"General" Comparison Methods

Cowell [11] presents a family of methods for comparing compact heat transfer surface configurations that is meant to overcome certain shortcomings of previous performance comparison methods. A group of comparison procedures are provided here that allow quantitative

evaluation of the important performance characteristics by the consideration of a range of parameters, without reference to any particular set of fluid properties and flow rates.

A number of assumptions were made in developing these "general" comparison methods. First of all, this analysis considers the behavior of only one side of the heat exchanger. The thermal resistance between the other fluid and its surface is assumed to be zero, just like in the study of PEC conducted by Bergles, Blumenkrantz, and Taborek [14], [15]. Secondly, the effects of fin efficiency are ignored. Thirdly, it is assumed that all fluid properties can be identified by single values that are constant throughout the heat exchanger matrix. And finally, contraction and expansion losses at the matrix inlet and outlet are ignored.

The comparison methods developed by Cowell deal with five parameters of interest for compact heat transfer surfaces: hydraulic diameter, frontal area, total volume, pumping power, and number of transfer units. The table shown in Figure 22 provides equations that can be used to calculate relative values of one of the five parameters listed above when any of the other two are held constant. In Figure 22, the superscript "*" denotes the parameter that is being solved for, the superscript "+" denotes the parameters that are fixed, and "σ" is the ratio of the minimum free flow area to frontal area. Figure 22 can be used to make comparisons for fixed or variable heat duty, depending on which parameters are held constant.

Furthermore, the table in Figure 23 can be used to calculate parameter ratios relative to a reference surface when certain combinations of three of the other parameters are held constant. Here, the subscript "o" refers to a selected reference surface. Cowell [11] demonstrates how Figure 23 "provides simple and compact statements of the relative merit of different heat transfer surfaces."

The family of relationships given in Figures 22 and 23 can be used to compare compact heat transfer surfaces for a large number of conditions. However, because certain assumptions were made to ensure the simplicity of these methods, Cowell [11] explains, "For detailed comparisons between heat exchangers for a particular duty, the general methods can be used as indicators in the first instance, but the effects of the limiting assumptions must be evaluated."

Second Law Performance Evaluation Criteria

Recently, there have been a number of methods for evaluating heat transfer enhancement which employ the principles of second law analysis as well as those of first law analysis. These methods focus on entropy production and the destruction of useful energy (exergy) that results from heat transfer enhancement, and they are all founded on the same basic principle. That is, the use of heat transfer enhancement devices reduces the destruction of exergy due to heat transfer across a finite temperature difference, but it increases the exergy destruction due to fluid flow friction. Thus, the aim of all second law criteria is to minimize the net exergy destruction or the net entropy generation resulting from heat transfer enhancement.

Bejan and Pfister [18] use entropy generation as a measure of the relative merit of heat transfer enhancement techniques. The parameter which they use to describe the effect of augmentation on irreversibility is the "augmentation entropy generation number" ($N_{S,a}$), defined as:

$$N_{S,a} = S_a^{'}/S_o^{'} \qquad (19)$$

where $S_a^{'}/S_o^{'}$ is the ratio between the rate of entropy generation in an augmented duct ($S_a^{'}$) and the rate of entropy generation in an unaugmented reference duct ($S_o^{'}$).

The entropy generation rate in the reference duct can be written as:

$$S'_o = S'_{\Delta P,o} + S'_{\Delta T,o} \tag{20}$$

where: $S'_{\Delta P,o}$ = rate of entropy generation due to friction

$S'_{\Delta T,o}$ = rate of entropy generation due to heat transfer across a finite temperature difference

Bejan and Pfister then define the "irreversibility distribution ratio" (ϕ_o) as:

$$\phi_o = S'_{\Delta P,o} / S'_{\Delta T,o} \tag{21}$$

Substituting in ϕ_o, Equation 19 can be rewritten as:

$$N_{S,a} = N_{S,\Delta T} + \frac{\phi_o}{\phi_o + 1}\left(N_{S,\Delta P} - N_{S,\Delta T}\right) \tag{22}$$

where $N_{S,\Delta T}$ and $N_{S,\Delta P}$ are values attained by the augmentation entropy generation number ($N_{S,a}$) for the limits $\phi_o \rightarrow 0$ and $\phi_o \rightarrow \infty$, respectively:

$$N_{S,\Delta T} = \frac{S'_{a,\Delta T}}{S'_{o,\Delta T}} = \frac{St_o}{St_a}\frac{D_a}{D_o} \qquad N_{S,\Delta P} = \frac{S'_{a,\Delta P}}{S'_{o,\Delta P}} = \frac{f_a}{f_o}\frac{D_o}{D_a}\frac{A_o^2}{A_a^2} \tag{23,24}$$

where A is the flow cross-sectional area.

Bejan and Pfister [18] show that the thermodynamic merit of a given enhancement technique is linked to the irreversible operating mode of the apparatus, which is locally defined by ϕ_o. There is a marginal ϕ_o (usually below unity) which, when exceeded, leads to an increase in the rate of entropy generation, regardless of whether heat transfer is enhanced. Still, Bejan and Pfister state, "The task of selecting one technique over another is left to the designer, who must blend exergy conservation considerations with aspects such as ease of manufacture, maintenance, etc., into a comprehensive cost minimization procedure."

Chen and Huang [19] use the augmentation entropy generation number and the irreversibility distribution ratio as defined by Bejan and Pfister [18] in order to develop general evaluation criteria based on second-law analysis. This is done for two cases:

Case A. Reduce N_S for fixed basic geometry and flow rate
Case B. Reduce N_S for fixed basic geometry and pressure drop

Graphical results for Case A are shown in Figures 24 and 25. Graphical results for Case B are given in Figures 26 and 27. Note that the subscript "s" used in Figures 24-27 refers to a "smooth" or unaugmented reference surface, and is equivalent to the subscript "o" used in the above discussion of the entropy generation method. These figures "can be utilized to distinguish between the useful heat-transfer surfaces and unsuitable ones from the point of view of available energy." [19]

Zimparov and Vulchanov [20] present performance evaluation criteria (PEC) equations for enhanced heat transfer based on the entropy production theorem [18], [19] using the design constraints defined by Webb [17]. These equations, which are too numerous to go over here in any depth, generalize the PEC for enhanced heat transfer surfaces developed by first law analysis [14], [15], [17]. Zimparov and Vulchanov [20] say, "The general evaluation criteria may help to display inappropriate enhanced surfaces and assist the engineer to design better heat transfer equipment."

In essence, this method combines certain elements of all the first and second law methods for evaluating heat transfer enhancement that are discussed in this paper. It seems very likely that more work of this nature will be performed in the future. Also, criteria which blend first and second law analyses can be used to provide a thorough comparison of new methods of heat transfer enhancement that may be suggested to make heat exchangers more compact and efficient.

PLATE-FIN SURFACE GEOMETRIES

A large number of plate-fin geometries have been proposed for use in compact heat exchangers, and more are still being developed. A high-performance surface will enhance the heat transfer that takes place within the heat exchanger, without incurring penalties on friction and pressure drop that are severe enough to negate the benefits of heat transfer augmentation. In this section, the following types of plate-fin geometries are examined: plain fins, wavy and corrugated channels, offset-strip fins, louvered fins, and vortex generators.

Plain Fins

Plain fin surfaces are characterized by long uninterrupted flow passages with performance comparable to that obtained inside long circular tubes [5]. The plain fins that are most commonly used have flow channels with either a rectangular or triangular cross-section, corresponding to surfaces A and B in Figure 28. The enhancement in heat transfer achieved with plain fins is due mainly to increased area density, rather than any increase in the heat transfer coefficient [3]. Plain fins require a smaller flow frontal area than interrupted surfaces (i. e. offset strip fins and louvered fins) for given values of heat duty, pressure drop, and flow rate, but the flow length with plain fins will be greater, resulting in a higher overall heat exchanger volume [21].

Wavy and Corrugated Channels

Several studies have been conducted to evaluate the heat transfer enhancement provided by using wavy passages in compact heat exchangers. Numerous studies have also been conducted for corrugated channels that are essentially triangular wavy passages. O'Brien and Sparrow [22] conducted one of the first comprehensive studies of the heat transfer and friction characteristics for the fully developed region of a corrugated channel with $1500 < Re < 25{,}000$. Heat transfer for the corrugated channel shown in Figure 29 was enhanced by a factor of ~2.5 compared to a conventional straight channel, but the pressure drop for the corrugated duct was significantly higher as well.

Wavy and corrugated channels both enhance heat transfer by promoting mixing due to complex recirculatory flows and boundary layer separation. However, less friction is expected in wavy channels because the sharp corners of the corrugated channel are not present.

Soland, *et al.* [12] compared all of the plate-fin surfaces listed in Figure 8, and determined that the best one based on their criteria was the 17.8-3/8W wavy surface shown in Figure 30.

Snyder, *et al.* [23] measured heat transfer rates and pressure drop for the thermally fully developed region of a "serpentine" channel with geometry similar to the 17.8-3/8W surface for $250 < Re < 10{,}000$. However, the serpentine channel was "carefully designed to minimize the extent

of flow separation." The serpentine channel (Figure 31) consists of 30 recursive arc circles with centerline radius of curvature R, peak-to-peak amplitude b, and periodicity length λ. Experiments performed using this channel revealed heat transfer enhancement of ~9 times that of a parallel plate channel for air.

Other investigations into wavy surface geometries have centered around channels like the one shown in Figure 32, which have sinusoidal walls, rather than walls comprised of recursive arcs. Nishimura, *et al.* [24] experimentally analyzed the performance of sinusoidal wavy channels for three different alignment "phases" of the walls for $100 < Re < 10{,}000$. They concluded that the channel with constant height (0^o phase lag) performed slightly better than a converging-diverging wavy channel (180^o phase lag).

Wang and Vanka [25] conducted a numerical analysis of flow through the converging-diverging sinusoidal channel shown in Figure 32 for $5 < Re < 750$. For $Re < 320$, laminar steady flow was observed. In this regime, the heat transfer enhancement relative to a straight parallel-plate channel was minimal, and the friction factors were doubled. For $Re > 320$, the flow became unsteady, and a significant increase in heat transfer was observed. Like most information on the performance of wavy walls, this suggests that wavy channels can be a useful geometry for heat transfer enhancement, but only if they are applied to the correct flow regime.

Offset Strip Fins

The offset strip fin geometry (Figure 28c) is one of the most widely-used enhanced surfaces in compact heat exchangers. The enhancement principle of the offset strip fin is illustrated by Figure 33. Basically, a laminar boundary layer develops on the short strip length, and is then dissipated in the wake region between strips. Typical strip lengths range from 3 to 6 mm, and offset strip fins are usually employed in the laminar regime [2]. The enhancement provided by offset strip fins results from an increase in both the effective surface area and the heat transfer coefficient [3].

Louvered Fins

Louvered fin surfaces (Figure 28d) are commonly used in automobile radiators. The louvered fin geometry consists of an interrupted surface similar to that of the offset-strip fin. However, the slit strips of louvered fins are not completely offset. Instead, the slit fin is rotated between 20^o and 60^o relative to the direction of the airflow. Most radiators use a louver strip width of 1.0 to 1.25 mm [2]. For equal strip width, the louvered fin geometry provides enhancement comparable to that of offset strip fins. Moreover, louvered fins are less expensive than offset strip fins for large-quantity production, because of their ease of manufacture using high-speed mass production technology [21].

Vortex Generators

A wing-type vortex generator plate is shown in Figure 28e. Vortex generators do not significantly change the effective heat transfer surface area of the plate, but they increase the heat transfer coefficient by creating longitudinally spiraling vortices which promote mixing between the wall and core regions of the flow [3]. Vortex generators are a relatively new type of enhancement device, and an optimum geometry has not yet been arrived at. There are any number of possibilities for different vortex generator surfaces, since one can vary the size, angle of attack, aspect ratio, and/or arrangement of the vortex generators.

Brockmeier, *et al.* [3] compare the performance of the delta-shaped wing-type vortex generator plate in Figure 28e with that of the four other types of plate-fin surfaces shown in Figure 28. The performance data used for these four surfaces (Types A, B, C, and D) were derived from experimental results, but the data for the vortex generator surface (Type E) was predicted numerically, due to the relative scarcity of quality experimental data for this configuration.

In making their comparative assessment of the plate-fin surfaces, Brockmeier, *et al.* [3] used the VG-1 performance criterion defined by Webb [2]. The objective defined by this criterion is reduced total transfer area for fixed pumping power, heat duty, and mass flow rate. Also, the hydraulic diameter is held constant in order to eliminate its effects on the outcome of this comparison. The results are given in Figure 34, for $500 < Re_o < 2000$, where Re_o is the reference Reynolds number. Surfaces B, C, D, and E were evaluated with respect to the rectangular plain fin surface (Type A), which was chosen as the reference surface.

From Figure 34, one can conclude that the vortex generator surface (Type E) provides the largest reduction in heat exchanger surface area, and thus, the largest reduction in heat exchanger volume for this criterion. It is followed by the offset strip fin (Type C) and louvered fin (Type D) surfaces. The curves for these two surfaces lie fairly close to each other. Surfaces C, D, and E all significantly reduce the required transfer area compared to the rectangular plain fin surface (Type A). The triangular plain fin surface is shown to be the least effective of the five configurations considered in this study.

CONCLUSION

This paper gives a detailed description of certain types of geometries that can be used to enhance heat transfer. Also, various methods of comparing the performance achieved by different types of enhanced surfaces applicable to compact heat exchangers were summarized.

Several plate-fin enhancement geometries have been developed in order to make heat exchangers more efficient and compact. Currently, plate-fin heat exchangers are very common in cryogenic systems and gas-liquefaction plants. Increased demand for smaller and better heat exchange devices will undoubtedly lead to more widespread use of plate-fin heat exchangers in other applications as well.

REFERENCES

1. A. E. Bergles, R. L. Webb and G. H. Junkan, Energy Conservation Via Heat Transfer Enhancement, *Energy,* Vol. 4, pp. 193-200, 1979.
2. R. L. Webb. Enhancement of Single-phase Heat Transfer, *Enhancement of Single-phase Heat Transfer.* S. Kakac, R. K. Shah, and A. E. Bergles ed. pp. 17-1-62 (Wiley, New York, 1987).
3. U. Brockmeier, T. Guentermann and M. Fiebig, Performance Evaluation of a Vortex Generator Heat Transfer Surface and Comparison with Different High Performance Surfaces, *International Journal of Heat and Mass Transfer,* Vol. 36, pp. 2575-2587, 1993.
4. R. K. Shah. Classification of Heat Exchangers, *Low Reynolds Number Flow Heat Exchangers.* S. Kakac, R. K. Shah, and A. E. Bergles ed. pp. 9-14 (Hemisphere Publishing Corporation, Washington, 1983).
5. W. M. Kays and A. L. London, *Compact Heat Exchangers*, The National Press, Palo Alto, CA, 1964.
6. P. G. LaHaye, F. J. Neugebauer and R. K. Sakhuja, A Generalized Prediction of Heat Transfer Surfaces, *Transactions of the ASME Journal of Heat Transfer,* Vol. 96, pp. 511-517, 1974.
7. R. H. Norris and W. A. Spofford, High Performance Fins for Heat Transfer, *Transactions of the ASME,* Vol. 64, pp. 489-496, 1942.

8. A. L. London, Compact Heat Exchangers, *Mechanical Engineering, ASME,* Vol. 86, pp. 31-34, 1964.

9. A. L. London and C. K. Ferguson, Test Results of High-performance Heat Exchanger Surfaces Used in Aircraft Intercoolers and Their Significance for Gas-turbine Regenerator Design, *Transactions of the ASME,* Vol. 71, pp. 17-26, 1949.

10. R. K. Shah and A. L. London, *Laminar Flow Forced Convection in Ducts*, Advances in Heat Transfer. J. Thomas F. Irvine and J. P. Hartnett ed. Academic Press, New York, 1978.

11. T. A. Cowell, A General Method for Comparison of Compact Heat Transfer Surfaces, *Transactions of the ASME Journal of Heat Transfer,* Vol. 112, pp. 288-294, 1990.

12. J. G. Soland, J. W. M. Mack and W. M. Rohsenow, Performance Ranking of Plate-Fin Heat Exchanger Surfaces, *Transactions of the ASME Journal of Heat Transfer,* Vol. 100, pp. 514-519, 1978.

13. D. F. Dipprey and R. H. Sabersky, Heat and Momentum Transfer in Smooth and Rough Tubes at Various Prandtl Numbers, *International Journal of Heat and Mass Transfer,* Vol. 6, 1963.

14. A. E. Bergles, A. R. Blumenkrantz and J. Taborek. *AIChE Preprint 9* (1972).

15. A. E. Bergles, A. R. Blumenkrantz and J. Taborek. *Paper FC6.3* (1974).

16. A. E. Bergles, R. L. Bunn and G. H. Junkhan, Extended Performance Evaluation Criteria for Enhanced Heat Transfer Surfaces, *Letters in Heat and Mass Transfer,* Vol. 1, pp. 113-120, 1974.

17. R. L. Webb, Performance Evaluation Criteria for Use of Enhanced Heat Transfer Surfaces in Heat Exchanger Design, *International Journal of Heat and Mass Transfer,* Vol. 24, pp. 715-726, 1981.

18. A. Bejan and Peter A. Pfister, Jr., Evaluation of Heat Transfer Augmentation Techniques Based on Their Impact on Entropy Generation, *Letters in Heat and Mass Transfer,* Vol. 7, pp. 97-106, 1980.

19. B. H. Chen and W. H. Huang, Performance-Evaluation Criteria for Enhanced Heat-Transfer Surfaces, *International Communications in Heat and Mass Transfer,* Vol. 15, pp. 59-72, 1988.

20. V. D. Zimparov and N. L. Vulchanov, Performance Evaluation Criteria for Enhanced Heat Transfer Surfaces, *International Journal of Heat and Mass Transfer,* Vol. 37, pp. 1807-1816, 1994.

21. R. K. Shah and R. L. Webb. Compact and Enhanced Heat Exchangers, *Heat Exchangers: Theory and Practice.* J. Taborek G. F. Hewitt, and N. Afgan ed. pp. 425-468 (Hemisphere Publishing Corporation, Washington, 1983).

22. J. E. O'Brien and E. M. Sparrow, Corrugated-Duct Heat Transfer, Pressure Drop, and Flow Visualization, *Transactions of the ASME, Journal of Heat Transfer,* Vol. 104, pp. 410-416, 1982.

23. B. Snyder, K. Li, and R. A. Wirtz, Heat Transfer Enhancement in a Serpentine Channel, *International Journal of Heat and Mass Transfer*, Vol. 36(12), pp. 2965-2976, 1993.

24. T. Nishimura, Y. Kajimoto and Y. Kawamura, Mass Transfer Enhancement in Channels with a Wavy Wall, *Journal of Chemical Engineering of Japan,* Vol. 19, pp. 142-144, 1986.

25. G. Wang and S. P. Vanka, Convective Heat Transfer in Periodic Wavy Passages, *International Journal of Heat and Mass Transfer* , Vol. 38, pp. 3219-3230, 1995.

26. A. G. Lenfestey, Low Temperature Heat Exchangers, *Cryogenics*, K. Mendelssohn ed. Vol. 3, pp. 23-48 (Heywood, London, 1961).

27. H. M. Joshi and R. L. Webb, Prediction of Heat Transfer in the Offset Strip Fin Array, *International Journal of Heat and Mass Transfer*, Vol. 30(1), pp. 69-84, 1987.

FIGURES

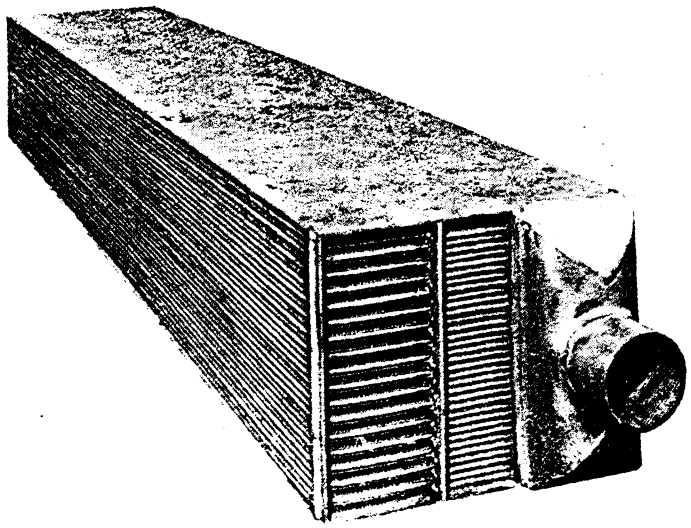

Fig. 1 Large matrix of plate-fin heat exchanger elements [26].

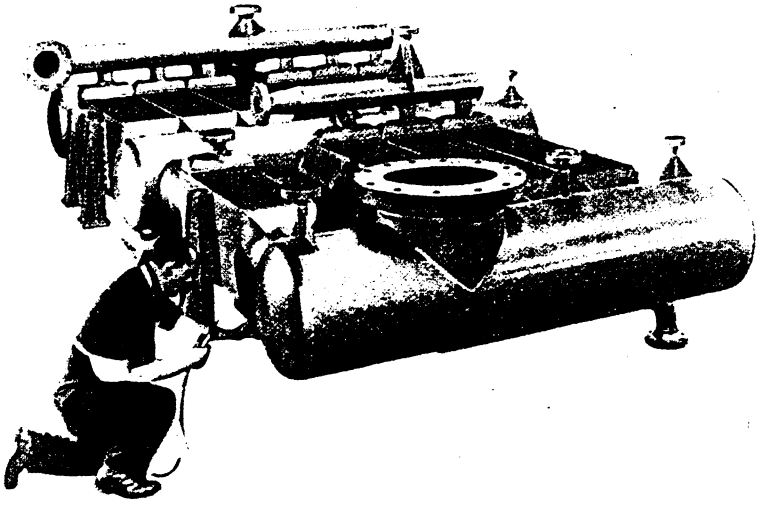

Fig. 2 Large plate-fin heat exchanger apparatus [26].

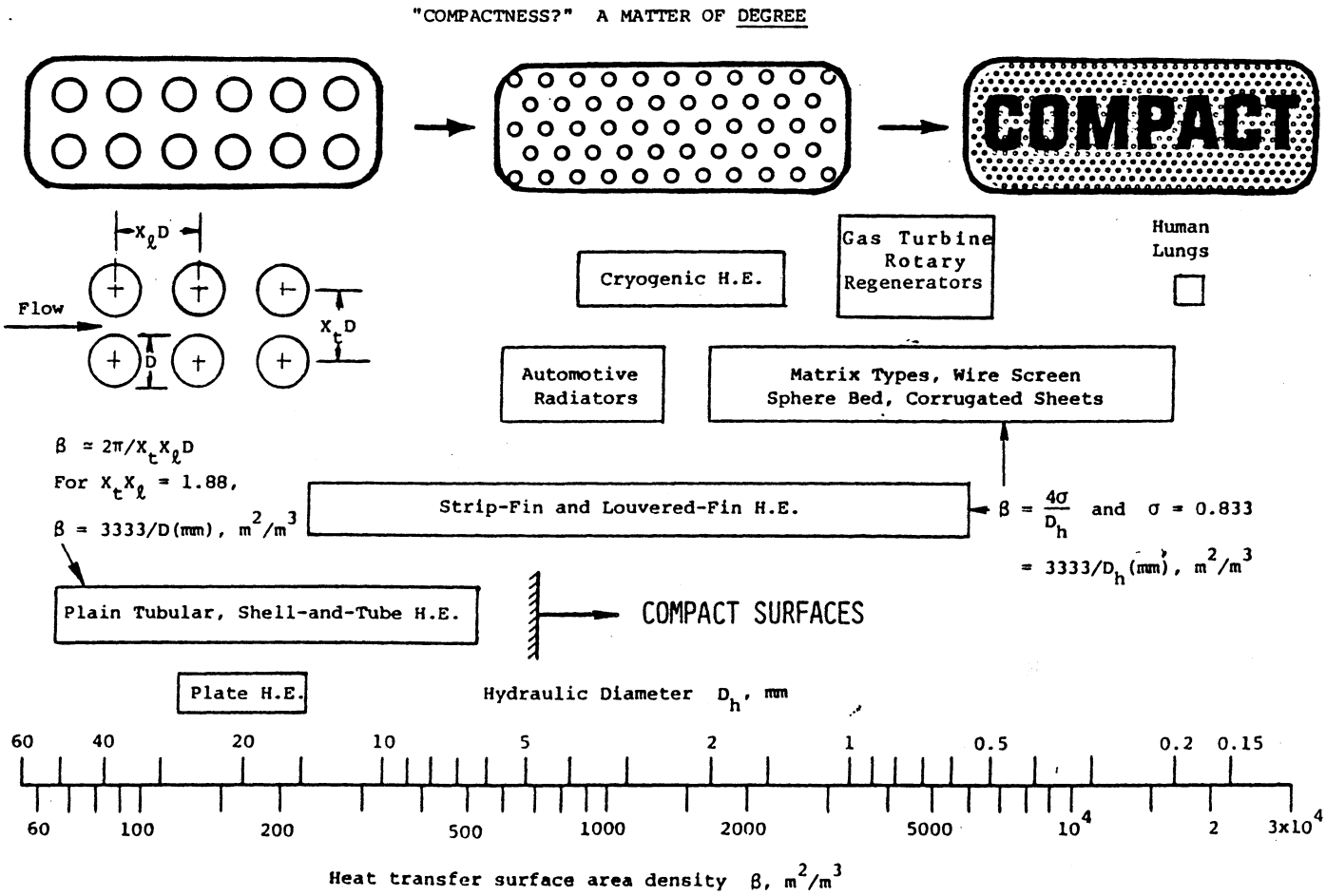

Fig. 3 Spectrum of surface area density for heat exchanger surfaces [4].

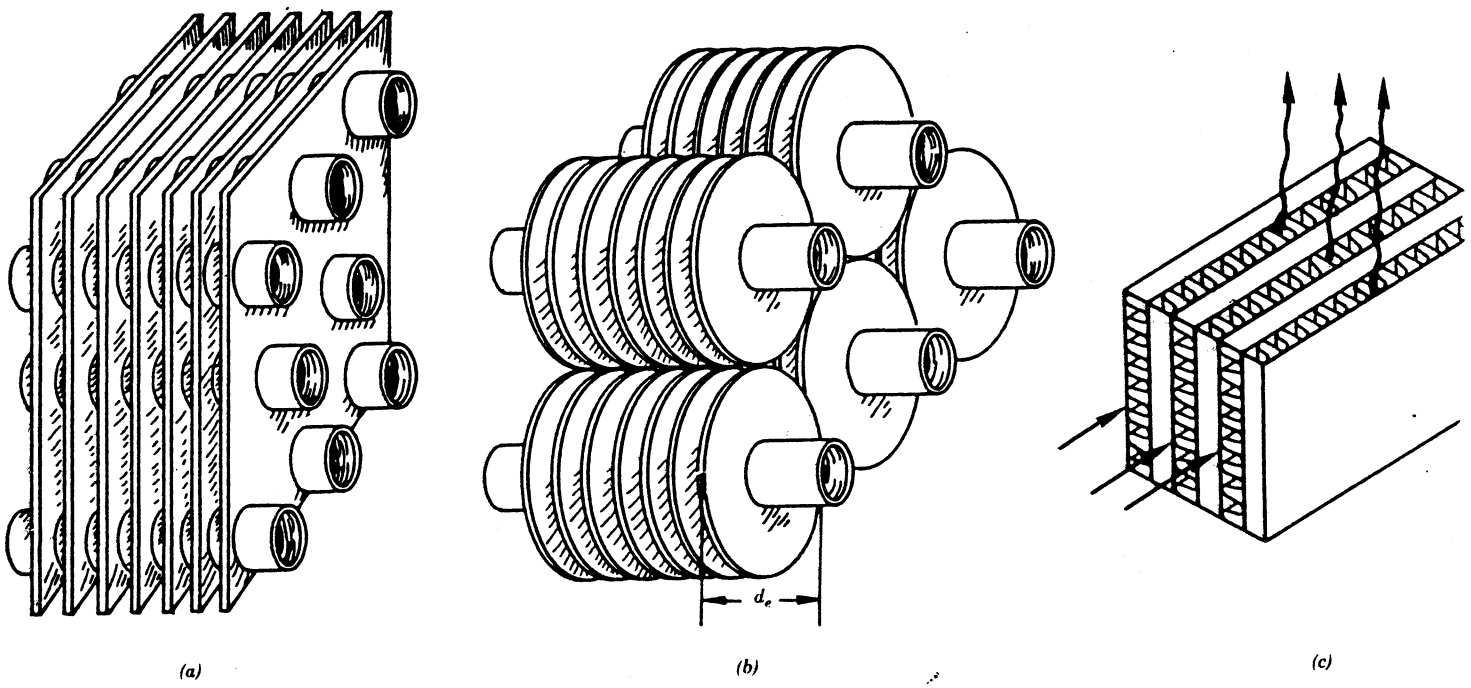

Fig. 4 (a) Finned-tube heat exchanger with flat fins, (b) individually finned tubes, (c) plate-fin heat exchanger [2].

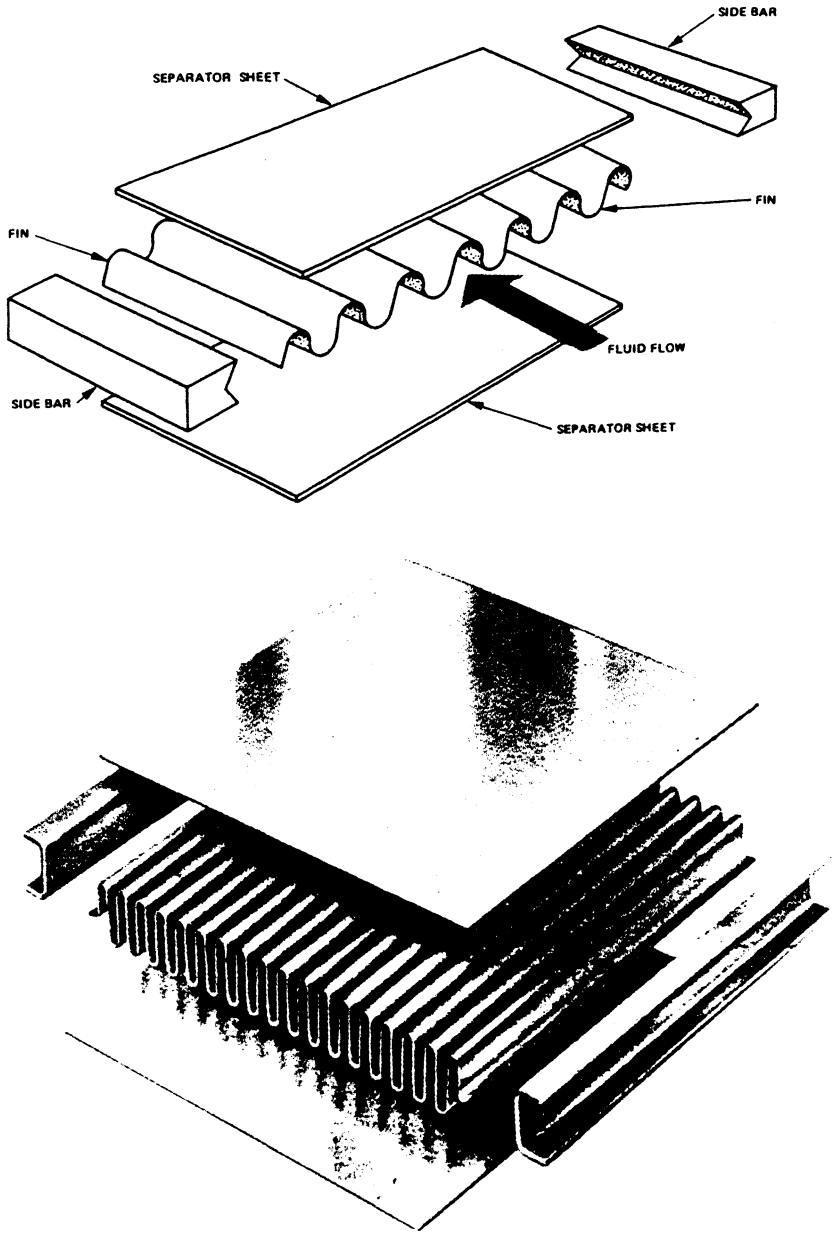

Fig. 5 Construction details of a typical single-element plate-fin heat exchanger [26].

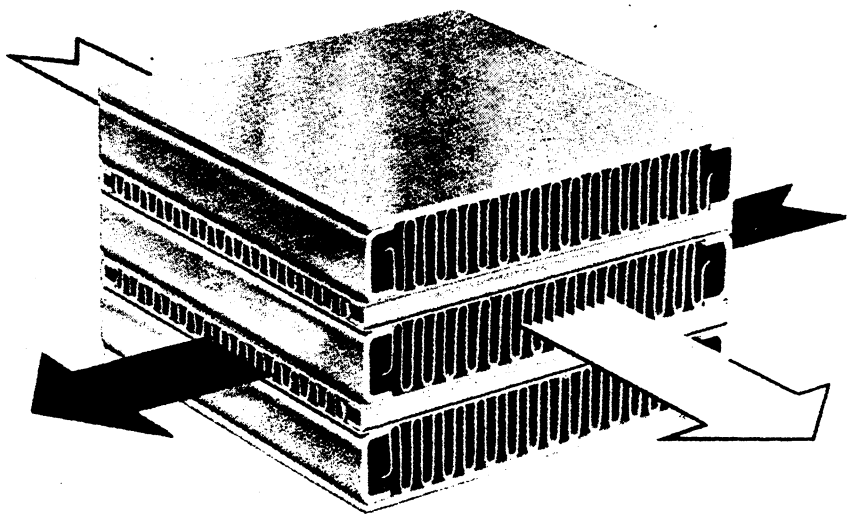

(a)

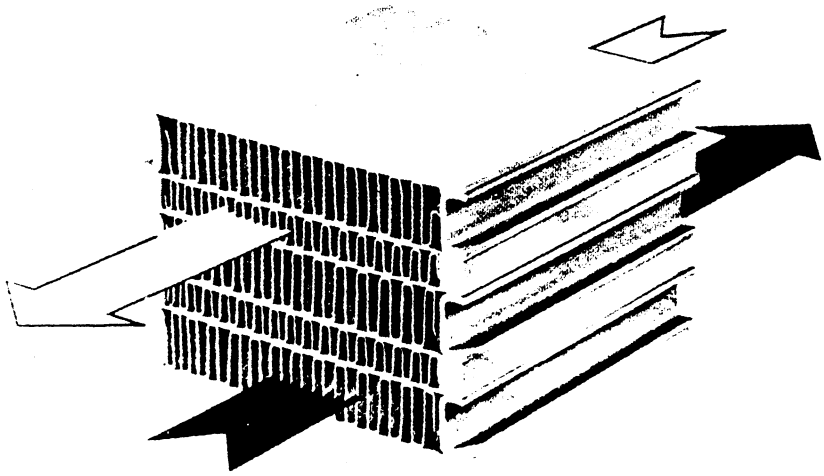

(b)

Fig. 6 (a) Crossflow and (b) counterflow arrangements of plate-fin heat exchangers [26].

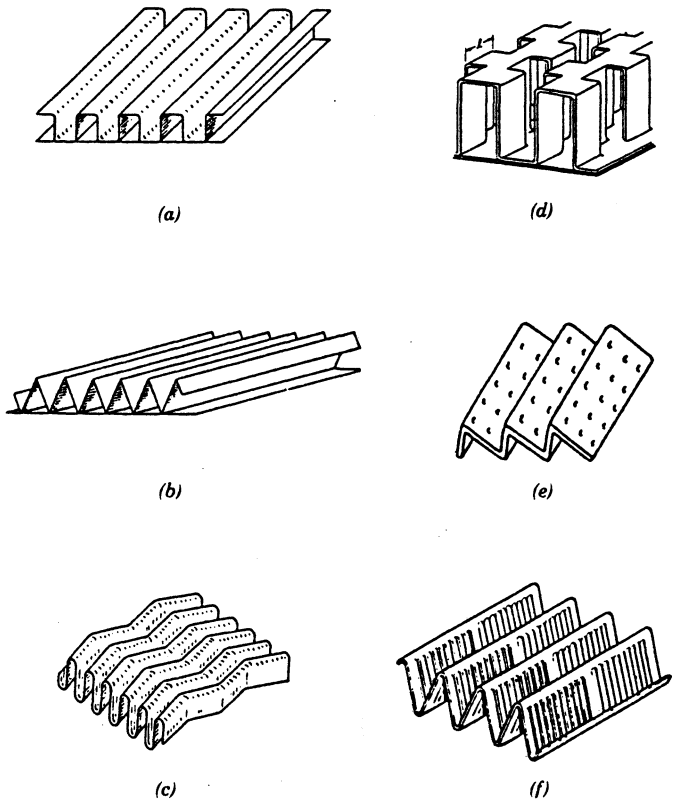

Fig. 7 (a) Plain rectangular fins, (b) plain triangular fins, (c) wavy fins, (d) offset strip fins, (e) perforated fins, (f) louvered fins [2].

(a) - PLAIN FINS

Surface Designation	Plate Spacing b ft.	Plate Spacing b in.	Fins per Inch	Hydraulic Diameter $4r_h$ ft.	Hydraulic Diameter $4r_h$ in.	Fin Thickness δ, in.	Flow Length of Uninterrupted Fin in.	Heat Transfer Area/ Volume Between Plates β ft^2/ft^3	Fin Area/ Total Area
4.00	0.015	0.180	See Surface Diagrams	0.0150	0.180	See Surface Diagrams	18.0	See Surface Diag.	0.500
5.3	0.0392	0.470	5.3	0.02016	0.242	0.006	2.49	188	0.719
6.2	0.0337	0.405	6.2	0.0182	0.218	0.010	1.20	204	0.728
9.03	0.0686	0.823	9.03	0.01522	0.1828	0.008	1.19	244	0.888
11.1	0.0208	0.250	11.1	0.01012	0.1213	0.006	2.50	367	0.756
11.11(a)	0.0400	0.480	11.11	0.01153	0.1385	0.008	8.00	312	0.854
14.77	0.0275	0.330	14.77	0.00848	0.1019	0.006	2.51	420	0.844
15.08	0.0348	0.418	15.08	0.00876	0.1052	0.006	6.84	414	0.870
19.86	0.0208	0.250	19.86	0.00615	0.0738	0.006	2.51	561	0.849

(b)- LOUVERED FINS

Surface Designation	Plate Spacing b ft.	Plate Spacing b in.	Fins per Inch	Hydraulic Diameter $4r_h$ ft.	Hydraulic Diameter $4r_h$ in.	Fin Thickness δ, in.	Louver Spacing in.	Louver Gap in.	Heat Transfer Area/ Volume Between Plates β ft^2/ft^3	Fin Area/ Total Area
3/8 - 6.06	0.0208	0.250	6.06	0.01460	0.1753	0.006	0.375	0.055	256	0.640
3/8(a)-6.06	0.0208	0.250	6.06	0.01460	0.1753	0.006	0.375	0.130	256	0.640
1/2 - 6.06	0.0208	0.250	6.06	0.01460	0.1753	0.006	0.500	0.055	256	0.640
1/2(a)-6.06	0.0208	0.250	6.06	0.01460	0.1753	0.006	0.500	0.130	256	0.640
3/8 - 8.7	0.0208	0.250	8.7	0.01196	0.1437	0.006	0.375	0.055	307	0.705
3/8(a)-8.7	0.0208	0.250	8.7	0.01196	0.1437	0.006	0.375	0.080	307	0.705
3/16 - 11.1	0.0208	0.250	11.1	0.01012	0.1214	0.006	0.1875	0.055	367	0.756
1/4 - 11.1	0.0208	0.250	11.1	0.01012	0.1214	0.006	0.250	0.035	367	0.756
1/4(b)-11.1	0.0208	0.250	11.1	0.01012	0.1214	0.006	0.250	0.055	367	0.756
3/8 - 11.1	0.0208	0.250	11.1	0.01012	0.1214	0.006	0.375	0.055	367	0.756
3/8(b)-11.1	0.0208	0.250	11.1	0.01012	0.1214	0.006	0.375	0.055	367	0.756
1/2 - 11.1	0.0208	0.250	11.1	0.01012	0.1214	0.006	0.500	0.055	367	0.756
3/4 - 11.1	0.0208	0.250	11.1	0.01012	0.1214	0.006	0.750	0.040	367	0.756
3/4(b)-11.1	0.0208	0.250	11.1	0.01012	0.1214	0.006	0.750	0.040	367	0.756

(c)-STRIP FINS

Surface Designation	Plate Spacing b ft.	Plate Spacing b in.	Fins per Inch	Hydraulic Diameter $4r_h$ ft.	Hydraulic Diameter $4r_h$ in.	Fin Thickness δ, in.	Flow Length of Uninterrupted Fin in.	Heat Transfer Area/ Volume Between Plates β ft^2/ft^3	Fin Area/ Total Area
1/4(s)-11.1	0.0208	0.250	11.1	0.01012	0.1214	0.006	0.25	367	0.756
3/32 - 12.2	0.0404	0.485	12.2	0.01120	0.1343	0.004	0.094	340	0.862
1/8 - 15.2	0.0348	0.414	15.2	0.00868	0.1042	0.006	0.125	417	0.873

(d)- WAVY FINS

Surface Designation	Plate Spacing b ft.	Plate Spacing b in.	Fins per Inch	Hydraulic Diameter $4r_h$ ft.	Hydraulic Diameter $4r_h$ in.	Fin Thickness δ, in.	Wave Length in.	Double Wave Amplitude, in.	Heat Transfer Area/ Volume Between Plates β ft^2/ft^3	Fin Area/ Total Area
11.48-3/8W	0.0345	0.413	11.44	0.01060	0.1272	0.006	0.375	0.0775	351	0.847
17.8 -3/8W	0.0345	0.413	17.8	0.00696	0.0836	0.006	0.375	0.0775	514	0.892

(e)-PIN FINS

Surface Designation	Plate Spacing b ft.	Plate Spacing b in.	Pin Pattern	Hydraulic Diameter $4r_h$ ft.	Hydraulic Diameter $4r_h$ in.	Pin Diameter in.	Transverse Pin Spacing, in.	Longitudinal Pin Spacing, in.	Heat Transfer Area/ Volume between plates β ft^2/ft^3	Fin Area/ Total Area
AP-1	0.020	0.240	In-Line	0.01444	0.1734	0.040	0.125	0.125	188	0.512
AP-2	0.0332	0.398	In-Line	0.01172	0.1408	0.040	0.12	0.096	204	0.686
PF-3	0.0625	0.750	In-Line	0.00536	0.0644	0.031	0.0602	0.0602	339	0.834
PF-4	0.0418	0.502	Staggered	0.0186	0.223	0.065	0.199	0.125	140	0.704
PF-9	0.0425	0.510	In-Line	0.0297	0.356	0.065	0.238	0.196	96.2	0.546

Fig. 8 Table of plate-fin surface geometries [5].

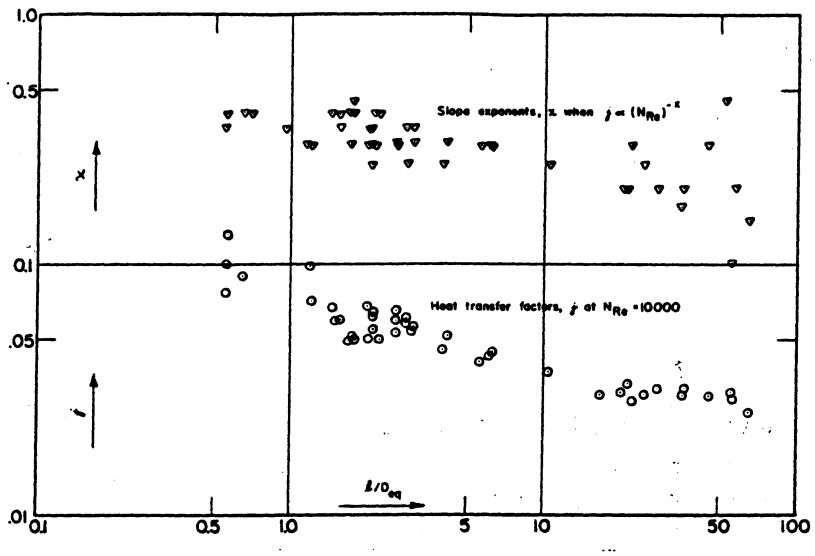

Fig. 9 Colburn factors (j) and their slope exponents versus specific flow length between major boundary layer disturbances [6].

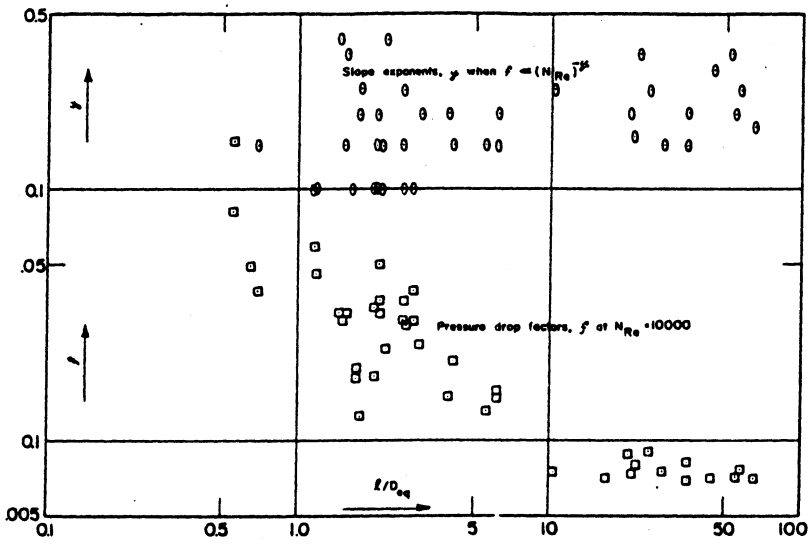

Fig. 10 Friction factors (f) and their slope exponents versus specific flow length between major boundary layer disturbances [6].

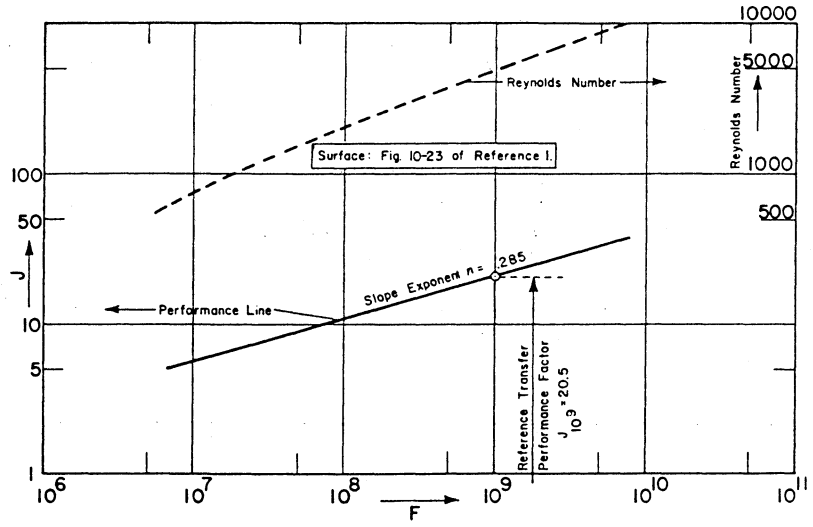

Fig. 11 Example of a dimensionless performance plot [6].

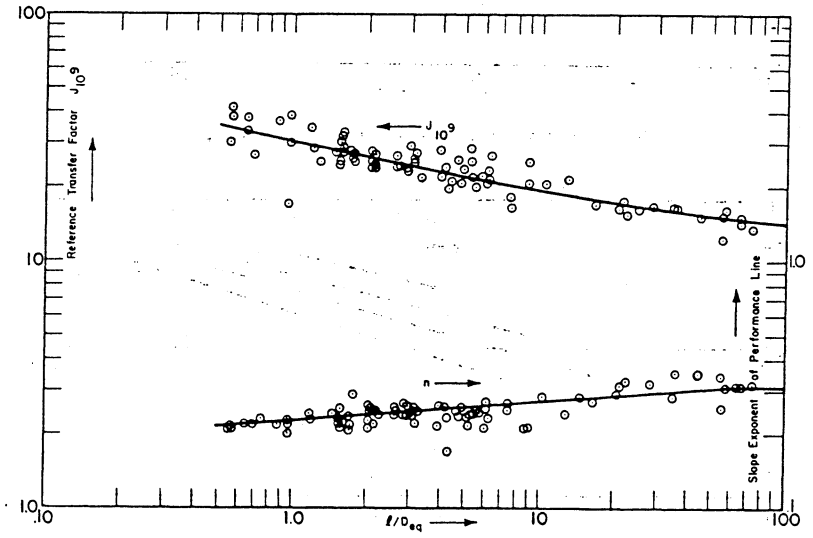

Fig. 12 Characteristics of the dimensionless performance plot versus specific flow length between major boundary layer disturbances [6].

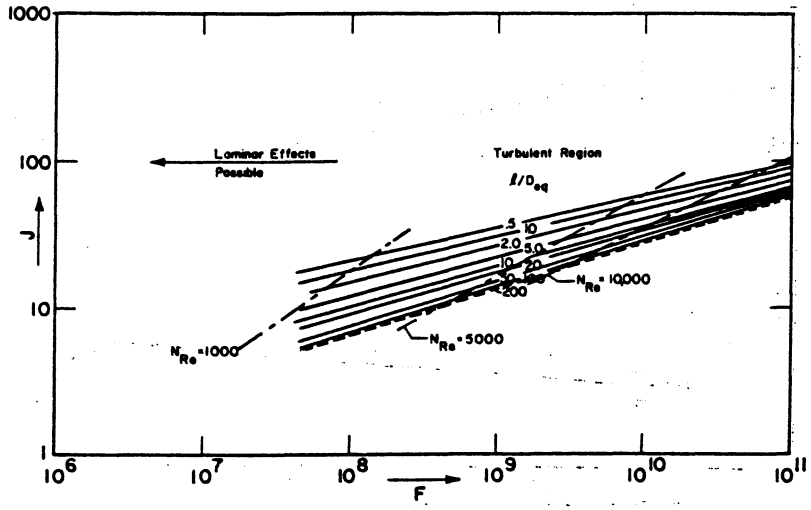

Fig. 13 Idealized dimensionless performance plot [6].

Kays and London [5]		Proposed	
$r_h \equiv \frac{A_c L}{A_T}$	(1a)	$D_n \equiv \frac{4A_F L}{A_b} = \frac{4V}{A_b}$	(1b)
$G_c \equiv \frac{\omega}{A_c}$	(2a)	$G_n \equiv \frac{\omega}{A_F}$	(2b)
$\mathrm{Re} \equiv \frac{4G_c r_h}{\mu}$	(3a)	$\mathrm{Re}_n \equiv \frac{G_n D_n}{\mu}$	(3b)
$f \equiv \frac{\Delta p_F}{\frac{L}{r_h}\frac{G_c^2}{2\rho g_0}}$	(4a)	$f_n \equiv \frac{\Delta p_F}{4\frac{L}{D_n}\frac{G_n^2}{2\rho g_0}}$	(4b)
$h \equiv \frac{q/\eta_0 A_T^*}{\Delta T}$	(5a)	$h_n \equiv \frac{q/A_b}{\Delta T}$	(5b)
$\mathrm{Nu} \equiv \frac{4r_h h}{k}$	(6a)	$\mathrm{Nu}_n \equiv \frac{h_n D_n}{k}$	(6b)
$j \equiv \frac{h}{G_c c_p}(\mathrm{Pr})^{2/3}$	(7a)	$j_n \equiv \frac{h_n}{G_n c_p}(\mathrm{Pr})^{2/3}$	(7b)
$^* \eta_0 \equiv \frac{A_{\mathrm{fin}}}{A_T}(1-\eta_f)$	(8)		
$\eta_f \equiv \frac{\tanh m\ell}{m\ell}$	(9)		
$m \equiv \sqrt{\frac{2}{\delta}\frac{h}{k_m}}$	(10a) thin sheet fins		
$m \equiv \sqrt{\frac{4}{\psi}\frac{h}{k_m}}$	(10b) circular pin fins		

Fig. 14 Equations for conversion of standard j and f vs. Re data [12].

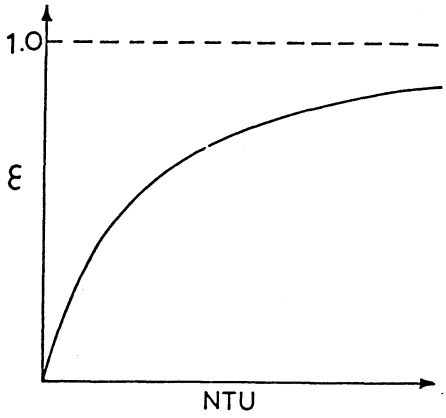

Fig. 15 Typical plot of heat exchanger effectiveness vs. number of transfer units [12].

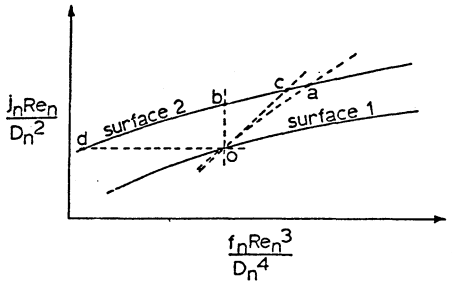

Fig. 16 Performance parameter curves for two surfaces showing points used in sample comparisons [12].

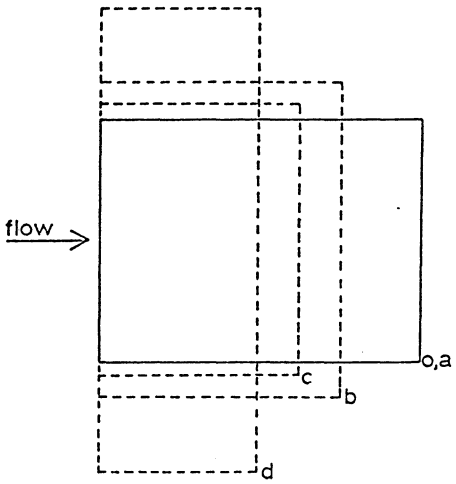

Fig. 17 Relative heat exchanger shape for sample comparisons assuming unit height [12].

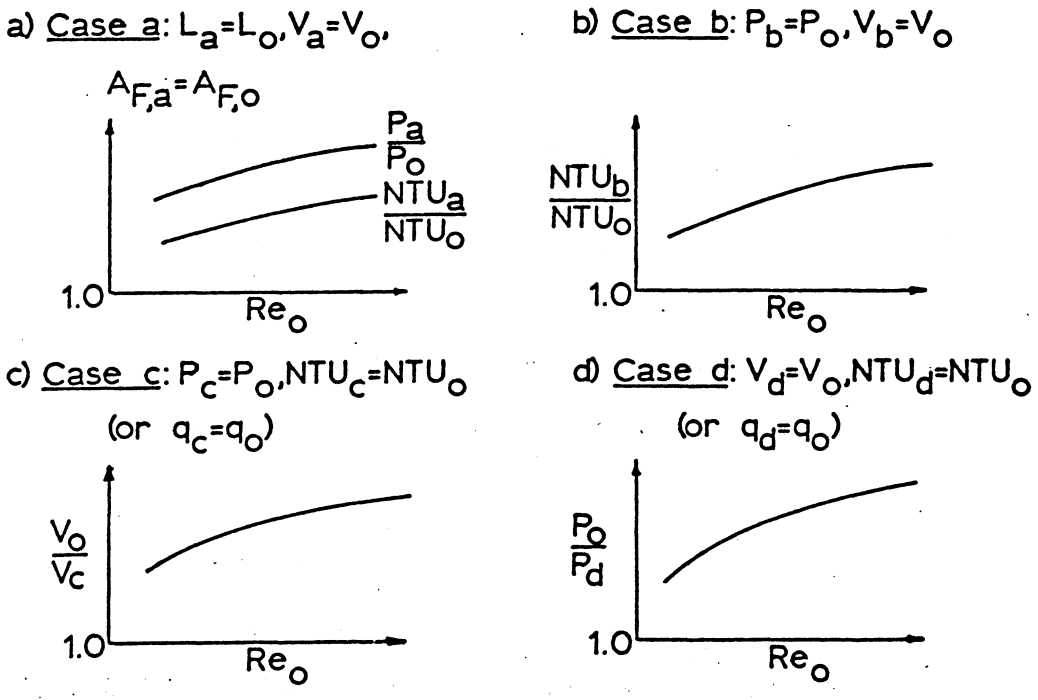

Fig. 18 Typical performance comparison results [12].

		Criterion Number							
		1	2	3	4	5	6	7	8
Fixed	Basic Geometry	X	X	X	X				
	Flow Rate	X						X	X
	Pressure Drop		X				X		X
	Pumping Power			X		X			
	Heat Duty				X	X	X	X	X
Objective	Increase Heat Transfer	X	X	X					
	Reduce Pumping Power				X				
	Reduce Exchanger Size					X	X	X	X

Fig. 19 Summary of Performance Evaluation Criteria [15].

Criterion	R_{ext}	Fixed							Objective
		basic geometry	w	Δp	P	T_{in}	ΔT	q	
1a	0	x	x			x	x		Increase heat duty
1b	0	x	x			x			"
1c	✓	x	x			x			"
2a	0	x		x		x	x		"
2b	0	x		x		x			"
2c	✓	x		x		x			"
3a	0	x			x	x	x		"
3b	0	x			x	x			"
3c	✓	x			x	x			"
4a	0	x				x	x	x	Reduce pumping power
4b	0	x				x		x	"
4c	✓	x				x		x	"

Fig. 20 Summary of Performance Evaluation Criteria [16].

Case	Fixed: Geom	W	P	q	ΔT_i	Objective	Consequences: $\frac{N}{N_p}$	$\frac{L}{L_p}$	$\frac{W}{W_p}$	$\frac{\mathrm{Re}}{\mathrm{Re}_p}$	$\frac{P}{P_p}$	$\frac{q}{q_p}$	$\frac{T_i}{T_{ip}}$
FG-1a	N, L	×			×	$\uparrow q$	1	1	1	1[b]	> 1	< 1	1
FG-1b	N, L	×		×		$\downarrow \Delta T_i$	1	1	1	1[b]	1	1	> 1
FG-2a	N, L		×		×	$\uparrow q$	1	1	< 1	< 1	1	> 1	1
FG-2b	N, L		×	×		$\downarrow \Delta T_i$	1	1	< 1	< 1	1	1	< 1
FG-3	N, L			×	×	$\downarrow P$	1	1	< 1	< 1	< 1	1	1
FN-1	N		×	×	×	$\downarrow L$	1	< 1	< 1	< 1	1	1	1
FN-2	N	×		×	×	$\downarrow L$	1	< 1	1	1[b]	< 1	1	1
FN-3	N	×		×	×	$\downarrow P$	1	< 1	1	1[b]	< 1	1	1
VG-1		×	×	×	×	$\downarrow NL$	> 1[c]	< 1	1	< 1[c]	1	1	1
VG-2a	NL[a]	×	×		×	$\uparrow q$	> 1[c]	< 1	1	< 1[c]	1	> 1	1
VG-2b	NL[a]	×	×	×		$\downarrow \Delta T_i$	> 1[c]	< 1	1	< 1[c]	1	1	< 1
VG-3	NL[a]	×		×	×	$\downarrow P$	< 1	< 1	1	< 1[c]	< 1	1	1

[a] The product of N and L is constant in cases VG-2 and VG-3.
[b] For internal roughness. For internal fins, $\mathrm{Re}/\mathrm{Re}_p = D_h S/d_i S_p$.
[c] Roughness with high-Pr fluids may not result in $N/N_p < 1$ (or $\mathrm{Re}/\mathrm{Re}_p < 1$).

Fig. 21 Performance Evaluation Criteria for flow inside tubes of the same envelope diameter [2].

RELATIVE PARAMETER	CONSTANT OR FIXED PARAMETER: N_{tu}^+ d^+	N_{tu}^+ A^+	N_{tu}^+ V^+	N_{tu}^+ P^+	P^+ d^+	P^+ A^+	P^+ V^+	V^+ d^+	V^+ A^+
d^*	—	$\sigma \mathrm{Re}$	$(\sigma j \mathrm{Re})^{1/2}$	$\left(\frac{f\mathrm{Re}^2}{j}\right)^{1/2}$	—	$\sigma \mathrm{Re}$	$\left(\sigma \mathrm{Re}^3\right)^{1/4}$	—	$\sigma \mathrm{Re}$
A^*	$\frac{d}{\sigma \mathrm{Re}}$	—	$\left(\frac{j}{\sigma \mathrm{Re}}\right)^{1/2}$	$\left(\frac{f}{j\sigma^2}\right)^{1/2}$	$\frac{d}{\sigma \mathrm{Re}}$	—	$\left(\frac{f}{\sigma^3 \mathrm{Re}}\right)^{1/4}$	$\frac{d}{\sigma \mathrm{Re}}$	—
V^*	$\frac{d^2}{\sigma j \mathrm{Re}}$	$\frac{\sigma \mathrm{Re}}{j}$	—	$\frac{f\mathrm{Re}}{\sigma j^2}$	$\frac{d^4}{\sigma f \mathrm{Re}^3}$	$\frac{\sigma^3 \mathrm{Re}}{f}$	—	—	—
P^*	$\frac{f\mathrm{Re}^2}{j d^2}$	$\frac{f}{\sigma^2 j}$	$\frac{f\mathrm{Re}}{\sigma j^2}$	—	—	—	—	$\frac{\sigma f \mathrm{Re}^3}{d^4}$	$\frac{f}{\sigma^3 \mathrm{Re}}$
N_{tu}^*	—	—	—	—	$\frac{j d^2}{f \mathrm{Re}^2}$	$\frac{j\sigma^2}{f}$	$\left(\frac{\sigma j^2}{f \mathrm{Re}}\right)^{1/2}$	$\frac{\sigma j \mathrm{Re}}{d^2}$	$\frac{j}{\sigma \mathrm{Re}}$

Fig. 22 Relative parameter values with two parameters held constant [11].

	CONSTANT OR FIXED PARAMETERS: A^+, V^+, N_{tu}^+	A^+, V^+, P^+	A^+, V^+, d^+	A^+, d^+, N_{tu}^+
Re_o	$0.6\left(\frac{\sigma \mathrm{Re}}{j}\right)^{1/3}$	$0.96\left(\frac{\sigma^3 \mathrm{Re}}{f}\right)^{2/3}$	$\sigma \mathrm{Re} \frac{d_o}{d}$	$\sigma \mathrm{Re} \frac{d_o}{d}$
$\frac{d}{d_o}$	$1.65\left(\sigma \mathrm{Re} j^2\right)^{1/3}$	$1.04\left(\frac{\mathrm{Re} f^2}{\sigma^3}\right)^{1/3}$	—	—
$\frac{V}{V_o}$	—	—	—	$0.47\left(\frac{d^3}{\sigma j^2 d_o^3 \mathrm{Re}}\right)^{1/2}$
$\frac{P}{P_o}$	$\frac{f}{2\sigma^2 j}$	—	$1.06\left(\frac{f^2 d_o^3 \mathrm{Re}}{d^3 \sigma^3}\right)^{1/2}$	$\frac{f}{2\sigma^2 j}$
$\frac{N_{tu}}{N_{tu_o}}$	—	$\frac{2\sigma^2 j}{f}$	$2.13\left(\frac{\sigma j^2 d_o^3 \mathrm{Re}}{d^3}\right)^{1/2}$	—

Fig. 23 Parameter ratios and reference surface Reynolds number with three parameters held constant [11].

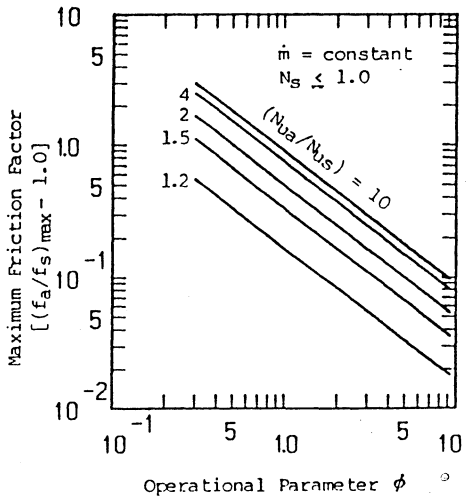

Fig. 24 Maximum friction factor vs. operational parameter [19].

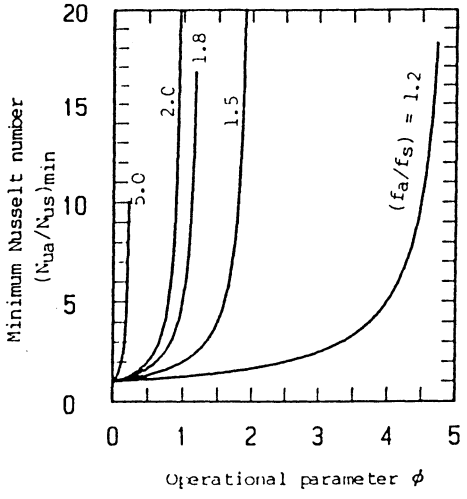

Fig. 25 Minimum Nusselt number vs. operational parameter [19].

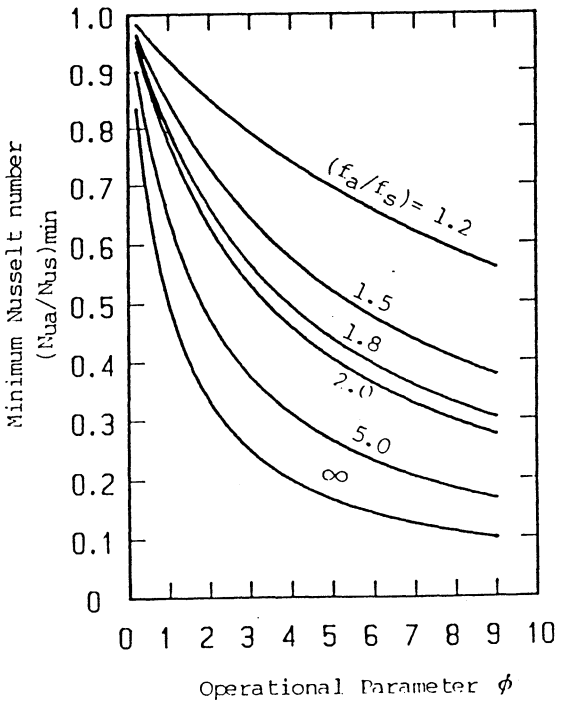

Fig. 26 Distribution of minimum Nusselt number [19].

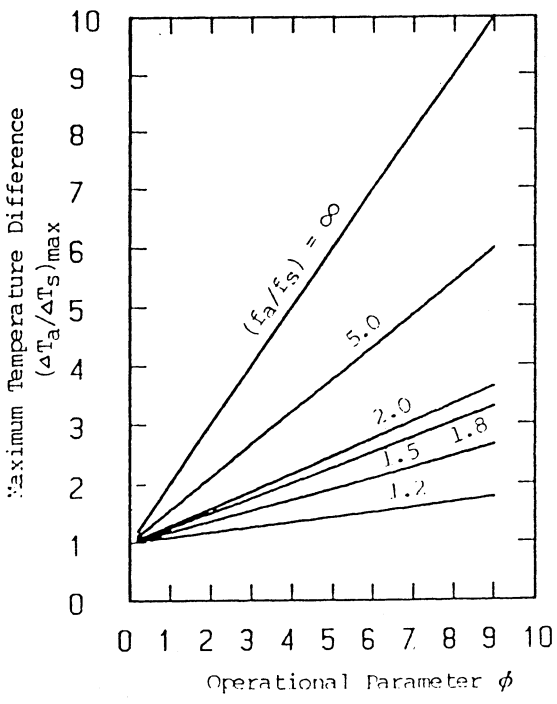

Fig. 27 Distribution of maximum temperature difference [19].

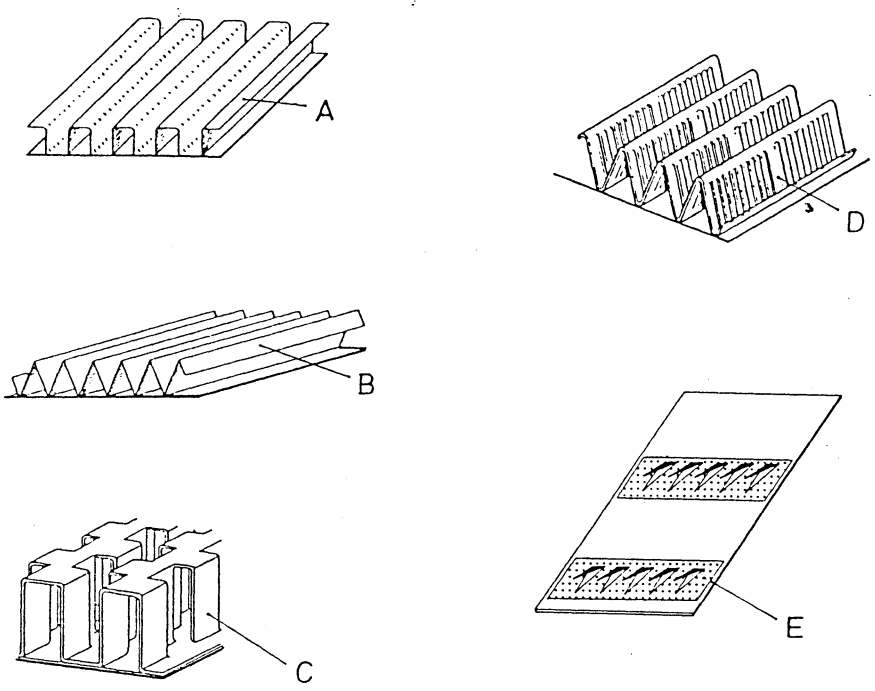

Fig. 28 (A) Rectangular plain fins, (B) triangular plain fins, (C) offset strip fins, (D) louvered fins, (E) vortex generators [3].

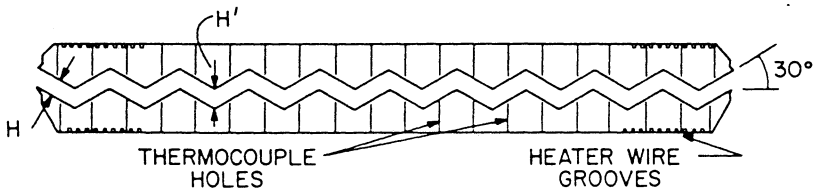

Fig. 29 Corrugated channel [22].

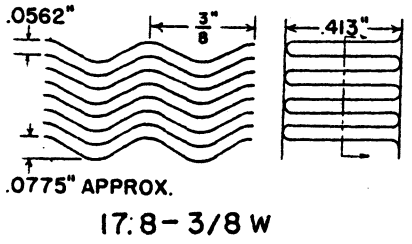

Fig. 30 17.8-3/8W wavy fin geometry [5].

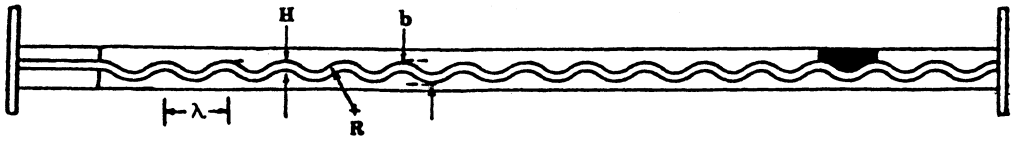

Fig. 31 "Serpentine" channel [23].

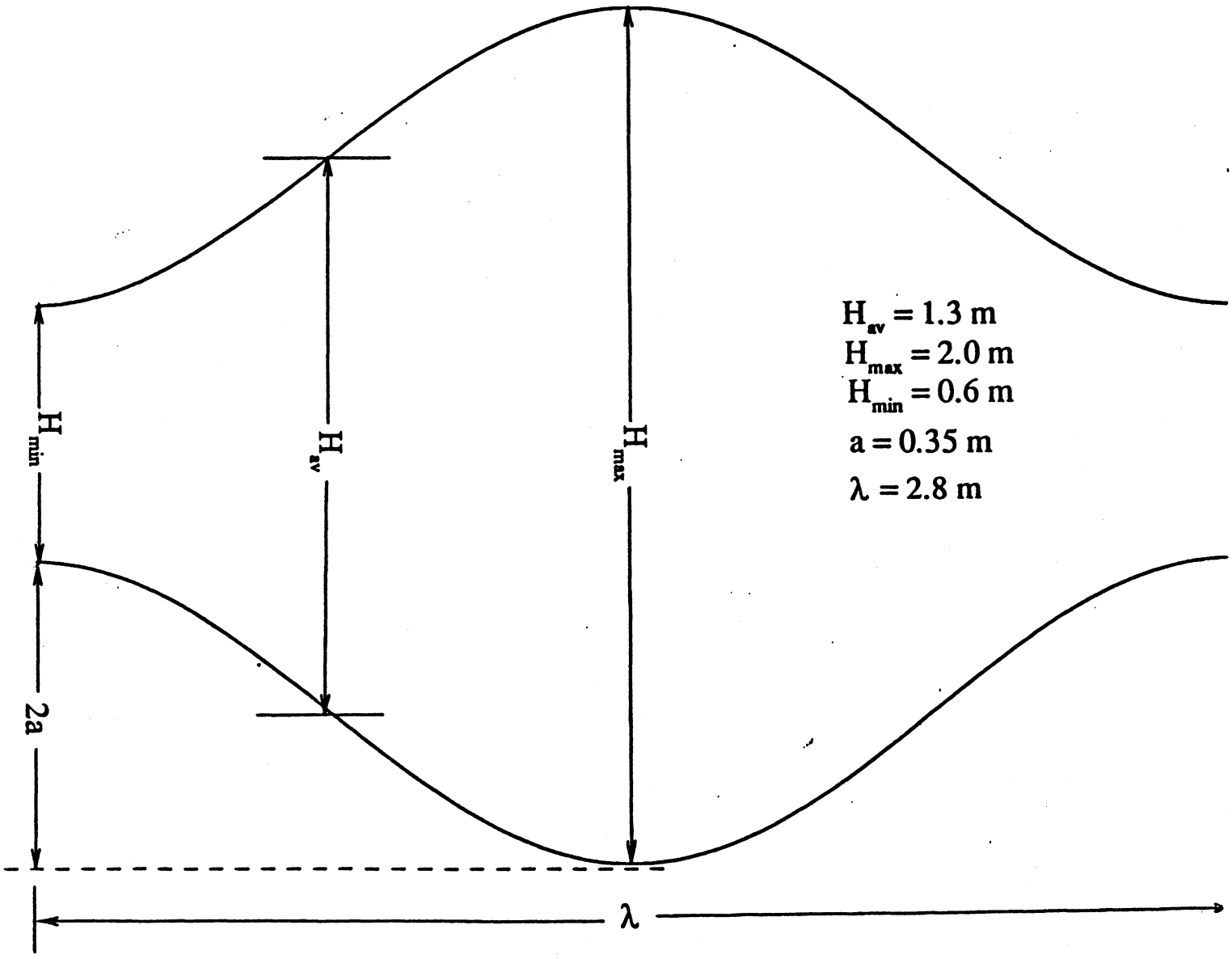

Fig. 32 Section of a sinusoidally curved wavy channel [25].